

# Accelerated waning of the humoral response to COVID-19 vaccines in obesity

Received: 9 August 2022

Accepted: 7 April 2023

Published online: 11 May 2023

 Check for updates

A list of authors and their affiliations appears at the end of the paper

Obesity is associated with an increased risk of severe Coronavirus Disease 2019 (COVID-19) infection and mortality. COVID-19 vaccines reduce the risk of serious COVID-19 outcomes; however, their effectiveness in people with obesity is incompletely understood. We studied the relationship among body mass index (BMI), hospitalization and mortality due to COVID-19 among 3.6 million people in Scotland using the Early Pandemic Evaluation and Enhanced Surveillance of COVID-19 (EAVE II) surveillance platform. We found that vaccinated individuals with severe obesity (BMI > 40 kg/m<sup>2</sup>) were 76% more likely to experience hospitalization or death from COVID-19 (adjusted rate ratio of 1.76 (95% confidence interval (CI), 1.60–1.94). We also conducted a prospective longitudinal study of a cohort of 28 individuals with severe obesity compared to 41 control individuals with normal BMI (BMI 18.5–24.9 kg/m<sup>2</sup>). We found that 55% of individuals with severe obesity had unquantifiable titers of neutralizing antibody against authentic severe acute respiratory syndrome coronavirus 2 (SARS-CoV-2) virus compared to 12% of individuals with normal BMI ( $P = 0.0003$ ) 6 months after their second vaccine dose. Furthermore, we observed that, for individuals with severe obesity, at any given anti-spike and anti-receptor-binding domain (RBD) antibody level, neutralizing capacity was lower than that of individuals with a normal BMI. Neutralizing capacity was restored by a third dose of vaccine but again declined more rapidly in people with severe obesity. We demonstrate that waning of COVID-19 vaccine-induced humoral immunity is accelerated in individuals with severe obesity. As obesity is associated with increased hospitalization and mortality from breakthrough infections, our findings have implications for vaccine prioritization policies.

Globally, obesity (defined as body mass index (BMI) > 30 kg/m<sup>2</sup>) is a major risk factor for severe Coronavirus Disease 2019 (COVID-19)<sup>1</sup>. Severe obesity (BMI > 40 kg/m<sup>2</sup>), which affects 3% of the population in the United Kingdom (UK) and 9% in the United States (US) (<https://www.worldobesity.org/>), is associated with a 90% higher risk of death from COVID-19 (ref. 2). Obesity is associated with type 2 diabetes mellitus, hypertension, chronic kidney disease and heart failure, comorbidities that may independently increase the risk of severe COVID-19 (refs. 3–7).

COVID-19 vaccines reduce the risk of symptomatic infection, hospitalization and mortality due to COVID-19 (refs. 8,9). They generate antibodies against the spike (S) protein of severe acute respiratory syndrome coronavirus 2 (SARS-CoV-2), comprising S1 and S2 subunits; S1 contains the receptor-binding domain (RBD), which mediates binding of the virus to angiotensin converting enzyme-2 (ACE-2) on host cells. The RBD is the main target for SARS-CoV-2 neutralizing antibodies, which inhibit viral replication in vitro and correlate with protection against infection in vivo<sup>10–12</sup>. As well as neutralizing antibodies,

✉ e-mail: [aziz.sheikh@ed.ac.uk](mailto:aziz.sheikh@ed.ac.uk); [isf20@cam.ac.uk](mailto:isf20@cam.ac.uk); [jedt2@cam.ac.uk](mailto:jedt2@cam.ac.uk)

**Table 1 | Policy summary**

Background	Obesity is associated with increased hospitalization and mortality due to severe COVID-19. Although COVID-19 vaccines are highly effective, details of the immune response and duration of vaccine efficacy in individuals with obesity are unknown.
Main findings and limitations	Using real-time data collected on over 3.6 million people in Scotland who had received two doses of primary COVID-19 vaccine, we show that the risk of severe COVID-19 is markedly increased (76%) in individuals with severe obesity (BMI > 40 kg/m <sup>2</sup> ). Breakthrough infections resulted in increased hospitalization and mortality due to COVID-19 and occurred more rapidly in individuals with severe obesity than in individuals with normal weight (after 10 weeks versus after 20 weeks), suggesting more rapid waning of protection. In an accompanying clinical study, we show that peak neutralizing antibody titers are similar in individuals with normal weight and individuals with severe obesity, indicating that the initial vaccine response is similar between the two groups. However, longitudinal immunophenotyping of both groups demonstrated that neutralizing capacity declines more rapidly in individuals with severe obesity. Although we did not observe an associated T cell defect, the number of individuals studied in the clinical cohort was modest, limiting the power to detect small differences.
Policy implications	Taken together, our results indicate that increased BMI affects the rate of decline of vaccine-mediated immunity against SARS-CoV-2 in the population. Given the high prevalence of obesity worldwide, these findings have major implications for vaccination policy globally. COVID-19 vaccines may need to be administered more frequently in individuals with severe obesity to achieve the duration of protection from severe COVID-19 that is seen in individuals with normal BMI. Furthermore, our demonstration that the kinetics of the adaptive immune response to vaccination differs in individuals with severe obesity has implications for immunization against other infectious diseases where the longitudinal vaccine response remains incompletely characterized. There is a pressing need to ensure appropriate demographic representation in clinical research studies and trials, which must seek to include individuals with varying degrees of obesity. Our work highlights the critical importance of collecting data on BMI and metabolic risk factors so that lessons can be learned rapidly to guide changes in policy and improve health outcomes.

non-neutralizing antibodies and cellular immunity contribute to protection, particularly against severe COVID-19. As immunity acquired after two doses of vaccine wanes over 6–9 months, many countries have elected to administer booster doses to maintain immune protection, particularly in older people and the immunocompromised<sup>13,14</sup>.

People with obesity have impaired immune responses to conventional influenza, rabies and hepatitis vaccines<sup>15–18</sup>; however, the effects of obesity on their responses to mRNA and adenoviral-vectored vaccines is not known. Several studies have suggested that, after COVID-19 vaccination, antibody titers may be lower in individuals with obesity than in the general population<sup>19–24</sup>. One possible explanation is the impact of needle length on vaccine dosing in individuals with obesity<sup>25</sup>, risking subcutaneous administration of a vaccine that is intended to be intramuscular. To date, longitudinal studies to investigate the duration of protection after COVID-19 vaccination in individuals with obesity have not been performed. Here we focus on individuals with severe obesity (those at highest risk). We conducted a prospective, longitudinal study that allowed us to demonstrate that, although initial and peak responses were similar in individuals with severe obesity and individuals with normal weight, there was accelerated decline in antibody levels over time that correlated with increased frequency of hospitalization and mortality from breakthrough infections. The findings and policy implications are summarized in Table 1.

## Results

### Severe COVID-19 outcomes in vaccinated individuals

To investigate the real-world effectiveness of COVID-19 vaccination in individuals with obesity, we used the Early Pandemic Evaluation and Enhanced Surveillance of COVID-19 (EAVE II) surveillance platform, which draws on near-real-time nationwide healthcare data for 5.4 million individuals (~99%) in Scotland, UK<sup>26–29</sup>. We interrogated data on 3,588,340 individuals aged ≥18 years who received a second dose (of the primary vaccination schedule) or a third booster dose of vaccine between 8 December 2020 and 19 March 2022 and were followed-up until hospitalization, death or the end of the study (19 March 2022; Table 2). BMI was recorded for 1,734,710 (49.2%) individuals who were included in the study. We first examined the effect of BMI on COVID-19-related hospitalization and mortality ≥14 d after receiving a second dose of either Pfizer-BioNTech BNT162b2 mRNA or AstraZeneca ChAdOx1 nCoV-19 vaccines. Between 14 September 2020 and 19 March 2022, there were 10,983 individuals (0.3%, 6.0 events per 1,000 person-years) who had a severe COVID-19 outcome: 9,733 individuals were hospitalized and 2,207 individuals died due to COVID-19 (957 individuals were hospitalized before their death).

**Table 2 | Population characteristics of individuals from EAVE II who received at least the second (of the primary vaccination schedule) or a third dose of a COVID-19 vaccine**

Characteristic	Total vaccination (n, %)	Severe COVID-19 outcome (n, rate per 1,000 person-years)
Total	3,588,340 (100.0)	10,938 (6.0)
Sex	Female	1,879,578 (52.4)
	Male	1,708,762 (47.6)
Age group (years)	18–49	1,634,424 (45.5)
	50–64	1,021,352 (28.5)
	65–79	706,617 (19.7)
	80+	225,947 (6.3)
BMI (kg/m <sup>2</sup> )	<18.5	36,197 (1.0)
	18.5–24.9	456,128 (12.7)
	25–29.9	2,428,889 (67.7)
	30–39.9	568,420 (15.8)
	40+	98,706 (2.8)

The frequency and rate per 1,000 person-years of severe COVID-19 outcomes (COVID-19-related hospitalization or death) was calculated. aRRs were estimated adjusting for all confounders, including age, sex, Scottish Index of Multiple Deprivation (SIMD), time since receiving the second dose of vaccine, number of pre-existing comorbidities, the gap between vaccine doses, previous history of SARS-CoV-2 infection and calendar time. Where the BMI was missing, it was imputed using ordinary least squares regression with all other independent variables included as predictors (BMI (imputed)).

Individuals with severe obesity (BMI > 40 kg/m<sup>2</sup>) were at increased risk of severe COVID-19 outcomes after a second vaccine dose compared to those with BMI in the normal range, with an adjusted rate ratio (aRR) of 1.76 (95% confidence interval (CI), 1.60–1.94) after adjusting for age, sex and socioeconomic status (Methods, Supplementary Data Tables 1–7 and Extended Data Figs. 1 and 2). A modest increase in risk was also seen in individuals who were obese (BMI 30–40 kg/m<sup>2</sup>) and those who were underweight (BMI < 18.5 kg/m<sup>2</sup>) (aRR 1.11, 95% CI 1.05–1.18 and aRR 1.28, 95% CI 1.12–1.47, respectively) (Supplementary Table 1). Individuals with obesity and severe obesity were at higher risk of hospitalization or death from COVID-19 after both a second (Fig. 1) and a third (booster) dose (Extended Data Fig. 1). Hospitalization and mortality from breakthrough infections after the second vaccine dose presented sooner in individuals with severe obesity (after 10 weeks; that is, 70 d) and obesity (after 15 weeks; that is, 105 d) than in individuals

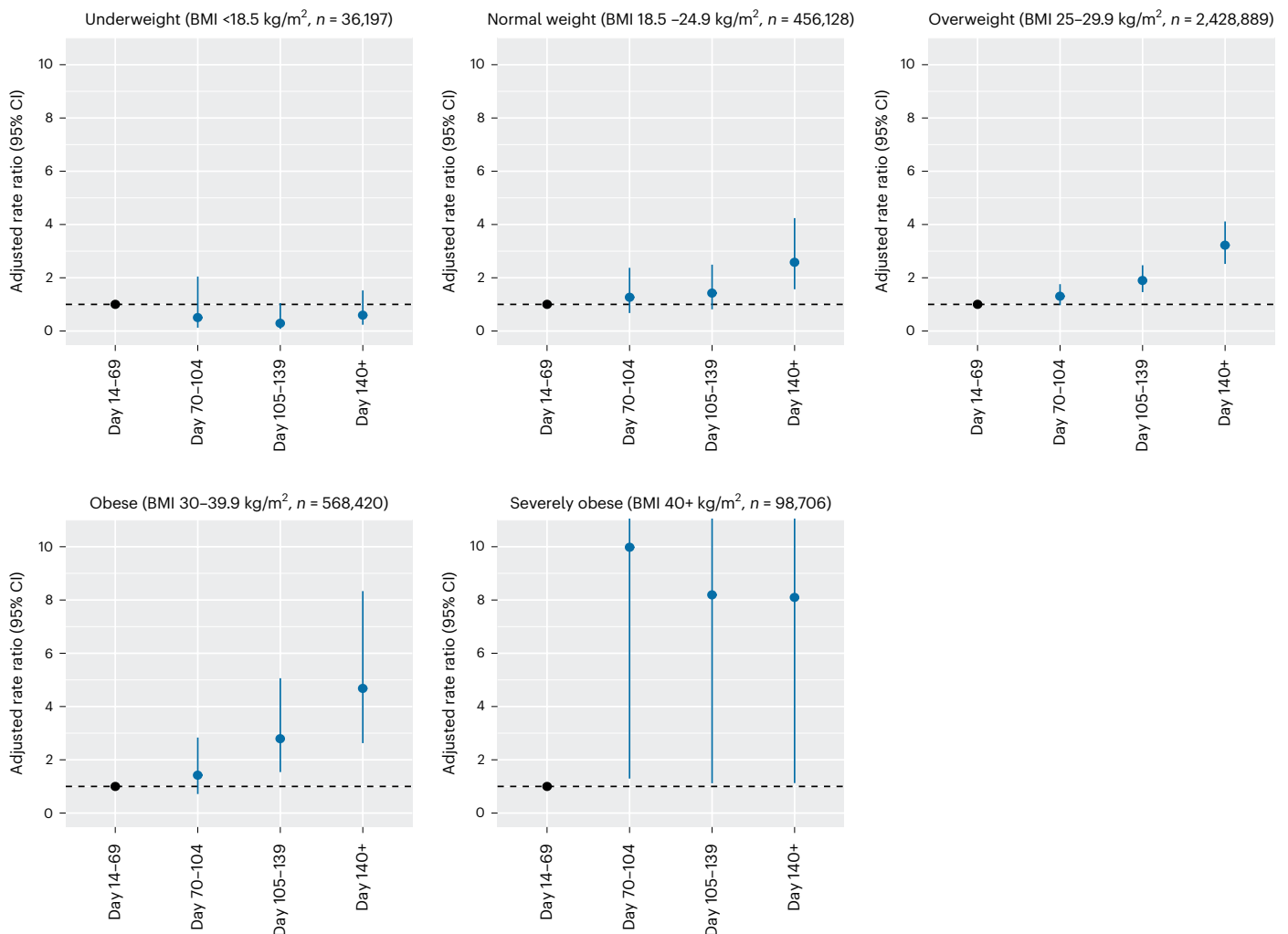


**Fig. 1 | Risk of severe COVID-19 outcomes after primary vaccination and relationship with BMI.** Panels depict the aRRs for hospitalization or death (severe COVID-19 outcomes) with time after the second COVID-19 vaccine dose for individuals in each BMI category in the EAVE-II cohort, Scotland. aRRs were estimated from five different models, one for each BMI category. aRRs were calculated against baseline risk at 14–69 d after the second vaccine dose. Error

bars indicate 95% CIs. The number (*n*) of individuals in each BMI category is indicated. Hospitalization and mortality from breakthrough infections after the second vaccine dose presented more quickly in individuals with severe obesity (after 10 weeks; that is, 70 d) and obesity (15 weeks; that is, 105 d) than in individuals with normal weight (20 weeks; that is, 140 d). aRRs are provided as mean with 95% CIs.

with normal weight (after 20 weeks; that is, 140 d) (Fig. 1 and Extended Data Fig. 1). A modest increase in risk was also seen for males in comparison to females (males versus females aRR 1.31, 95% CI 1.26–1.34).

Post hoc sensitivity analyses in clinically confirmed cases and after pooling the results of 10 imputations by chained equations generated very similar results (Supplementary Data Table 1). We found that vaccinated individuals with severe obesity and who had type 2 diabetes were at increased risk of admission to hospital or death due to COVID-19 (aRR 1.43, 95% CI 1.17–1.74; Extended Data Fig. 1f). A diagnosis of type 2 diabetes was independently associated with an increased risk of a severe COVID-19 outcome despite vaccination (aRR 1.13, 95% CI 1.07–1.19), although this was less than the risk associated with severe obesity. The aRR for type 2 diabetes was reduced slightly after adjusting for BMI (1.06, 95% CI 1.00–1.12).

### Immunity after primary vaccination in individuals with obesity

To investigate the effects of severe obesity on humoral and cellular immunity to COVID-19 vaccination, we performed prospective longitudinal immunophenotyping of a clinical cohort of individuals with severe obesity (*n* = 28) and normal BMI control individuals (*n* = 41) in

Cambridge, UK (SARS-CoV2 Vaccination Response in Obesity (SCORPIO) study) (Fig. 2 and Supplementary Data Table 8). All participants had received a two-dose primary course of COVID-19 vaccine approximately 6 months before study enrollment (Fig. 2a). As prior natural COVID-19 infection enhances subsequent vaccination responses, individuals with detectable anti-nucleocapsid antibodies (*n* = 2 with severe obesity; *n* = 1 normal BMI control) were excluded. Mean levels of anti-spike and anti-RBD IgG antibodies were similar between individuals with severe obesity and normal BMI 6 months after the second vaccine dose (Fig. 2b and Extended Data Fig. 3). By contrast, the function of these antibodies, measured by their ability to neutralize authentic SARS-CoV-2 viral infection (neutralizing titers at 50% inhibition ( $NT_{50}$ ))<sup>30</sup>, was reduced in individuals with severe obesity (Fig. 2c). Fifty-five percent of individuals with severe obesity had unquantifiable or undetectable neutralizing capacity compared to 12% of normal BMI controls ( $Z = 3.610$ ,  $P = 0.0003$ ,  $Z$ -test; Fig. 2d). Dissociation between anti-spike antibody levels and neutralizing capacity could be a consequence of lower antibody affinity or differential antibody reactivity to non-neutralizing epitopes on the spike protein. Here, the similar levels of RBD-binding antibodies across both groups indicate adequate capacity for antibody production against neutralizing epitopes and suggest a lower affinity of SARS-CoV-2

antibodies in individuals with severe obesity. Consistent with this observation, despite equivalent levels of anti-RBD antibodies, neutralizing capacity tended to be higher in individuals with a normal BMI (Extended Data Fig. 4). Baseline plasma glucose, leptin levels, diagnosis of type 2 diabetes or type of vaccine did not correlate with neutralizing capacity in individuals with severe obesity (Extended Data Fig. 3b–f).

Suboptimal antibody responses might be enhanced by activating memory B cells, which can rapidly differentiate into antibody-producing plasma cells after booster immunization. However, we found that circulating antigen-experienced (IgD<sup>+</sup>) RBD-binding B cells were similar in both groups ( $P = 0.1448$ ; Fig. 2e and Extended Data Fig. 3g,h). Antigen-specific T cell responses quantified by ELISpot were also similar in individuals with severe obesity and normal BMI controls (Extended Data Fig. 3i;  $P = 0.2243$  for V3D0, where V3D0 denotes vaccine 3 day 0 (sampling time-point before third dose)).

### Response to booster vaccination

We next studied the response to a third (booster) dose of mRNA vaccine (BNT162b2 or mRNA1273) in individuals with severe obesity ( $n = 28$ ) and individuals with normal BMI ( $n = 16$ ). As expected, levels of anti-spike and anti-RBD IgG antibodies increased markedly at day 28 (Fig. 3a and Extended Data Fig. 5). Peak levels were higher in individuals with severe obesity than in individuals with normal BMI ( $P = 0.0052$ , Fig. 3a and  $P = 0.0014$ , Extended Data Fig. 5a). Unlike anti-spike and anti-RBD antibody levels, neutralizing antibody titers were similar between the two groups at day 28 (Fig. 3b,  $P = 0.3534$ , and Extended Data Fig. 5b). Similar to the primary vaccine response, despite equivalent levels of anti-RBD antibodies, neutralizing capacity was higher in individuals with normal BMI (Extended Data Fig. 4b–f). Nonetheless, all individuals generated an  $NT_{50} > 100$ , and 61% ( $n = 17$ ) of individuals with severe obesity and 67% ( $n = 8$ ) of individuals with normal BMI generated an  $NT_{50} > 1,000$ .

To further assess humoral immunity associated with severe obesity, we next used an established high-dimensional spectral flow cytometry panel<sup>31</sup> to enumerate and phenotype SARS-CoV-2 RBD-binding B cells (Fig. 3c–e and Extended Data Fig. 6a–c). Unsupervised t-distributed stochastic neighbor embedding (tSNE) analysis of RBD-binding (RBD<sup>+</sup>) cells was performed on all IgD<sup>+</sup> B cells combined from individuals with normal BMI and individuals with severe obesity at several timepoints. Cluster 1 represented IgM<sup>+</sup> B cells; cluster 2 showed features of atypical or age-associated B cells<sup>32</sup>; cluster 3 separated plasmablasts; and the smallest clusters (4 and 5) were class-switched memory B cells (Fig. 3c–e). Cells from individuals with severe obesity and from individuals with normal BMI were distributed within all clusters, at all timepoints, suggesting that obesity was not associated with a loss of B cell subset differentiation. However, classical bi-axial gating identified that individuals with severe obesity had an increased frequency of IgD<sup>+</sup> CD71<sup>+</sup> RBD-binding B cells 8 d after the booster (Extended Data Fig. 6b,c). The number of circulating T follicular helper (cTfh) cells, a circulating biomarker of the germinal center reaction<sup>33</sup>, did not differ between the groups (Extended Data Fig. 6d–h). Consistent with this, antigen-specific T cell responses quantified by ELISpot and the number of regulatory T cells were similar in individuals with severe obesity and individuals with normal BMI (Extended Data Fig. 3i;  $P = 0.8173$  for V3D8 and  $P = 0.8903$  for V3D28).

### Waning of humoral immunity after booster vaccination

The lower neutralizing antibody titers observed in individuals with severe obesity before booster vaccination could reflect a reduction in either the peak response to primary vaccination or its longevity. We, therefore, measured antibody levels at day 28 and day 105 (15 weeks) after the third dose of vaccine. We found more rapid waning of anti-spike and anti-RBD IgG levels and neutralizing antibody titers in individuals with severe obesity ( $P = 0.0057$  for percentage change in anti-spike IgG;  $P = 0.0087$  for percentage change in anti-RBD IgG;  $P = 0.0220$  for percentage change in  $NT_{50}$ ; Fig. 4a–e). Neutralizing capacity against the Omicron variant of SARS-CoV-2 (BA.1) was similarly reduced with time (Extended Data Fig. 7). Conversely, antigen-specific T cell responses quantified by ELISpot remained similar in individuals with severe obesity and individuals with normal BMI at day 105 (Fig. 4f). Taken together, these data indicate that severe obesity leads to a failure in the maintenance of humoral immunity after COVID-19 vaccination, associated with an increased risk of severe COVID-19.

### Discussion

Obesity is an established risk factor for severe COVID-19 (ref. 2). In this study of over 0.5 million vaccinated individuals with obesity and more than 98,000 vaccinated individuals with severe obesity, we found that an increased BMI is associated with an increased risk of hospitalization and mortality from breakthrough infections. In parallel, we found evidence of reduced neutralizing antibody capacity 6 months after primary vaccination in individuals with severe obesity. These changes in antibody kinetics are associated with a dissociation between anti-RBD antibody levels and neutralizing capacity. A similar, relative reduction in neutralizing capacity was previously observed in patients with severe COVID-19 in other settings<sup>34,35</sup> and might reflect lower antibody affinities. Consistent with the kinetics of the neutralizing antibody response in individuals with severe obesity, we show an increased risk of severe outcomes of COVID-19 even after COVID-19 vaccination in individuals with severe obesity, which increases with time after the primary vaccination course.

Our findings in individuals with severe obesity are consistent with previous studies showing that COVID-19 vaccines are immunogenic in individuals with obesity and individuals with a normal BMI<sup>19–24</sup>. In addition, our finding that peak antibody levels were in fact higher in individuals with severe obesity than in individuals with a normal BMI argues against vaccine delivery failure in individuals with obesity due to short needle length<sup>25</sup> (longer needles are recommended for individuals with BMI > 40 kg/m<sup>2</sup> in the UK) and indicates that a fixed rather than a weight-adjusted dosing schedule is appropriate for COVID-19 vaccination. Some of these studies suggested that the duration of vaccine-induced immunity could be reduced in individuals with obesity<sup>20–22</sup>. These studies all relied on measurements of immunity at a single timepoint and used different assays and/or endpoints (for example, self-reported home antibody tests<sup>23</sup> or an assumption of effectiveness in those who tested negative for COVID-19 by RT-PCR<sup>24</sup>). Here, by prospectively measuring B cell and T cell responses as well as neutralizing capacity of antibodies to authentic virus in vaccinated individuals with severe obesity and normal BMI over time, we demonstrate that the waning of humoral immunity associated with COVID-19 vaccines<sup>36</sup> is

**Fig. 2 | COVID-19 vaccine-induced immunity in individuals with severe obesity and individuals with normal weight 6 months after primary vaccination.** **a**, Detailed longitudinal immunophenotyping studies were performed on individuals with severe obesity (magenta,  $n = 22$ ) and normal BMI control individuals (black,  $n = 46$ ). Samples were obtained 6 months after the second dose of COVID-19 vaccine (V2) administered as part of their primary vaccination course and at several timepoints after the third dose (V3) as indicated. **b**, Anti-spike IgG titers are similar in individuals with severe obesity ( $n = 22$ , magenta) and individuals with normal weight ( $n = 41$ , black) 6 months after primary vaccination course. Horizontal bars indicate the median and

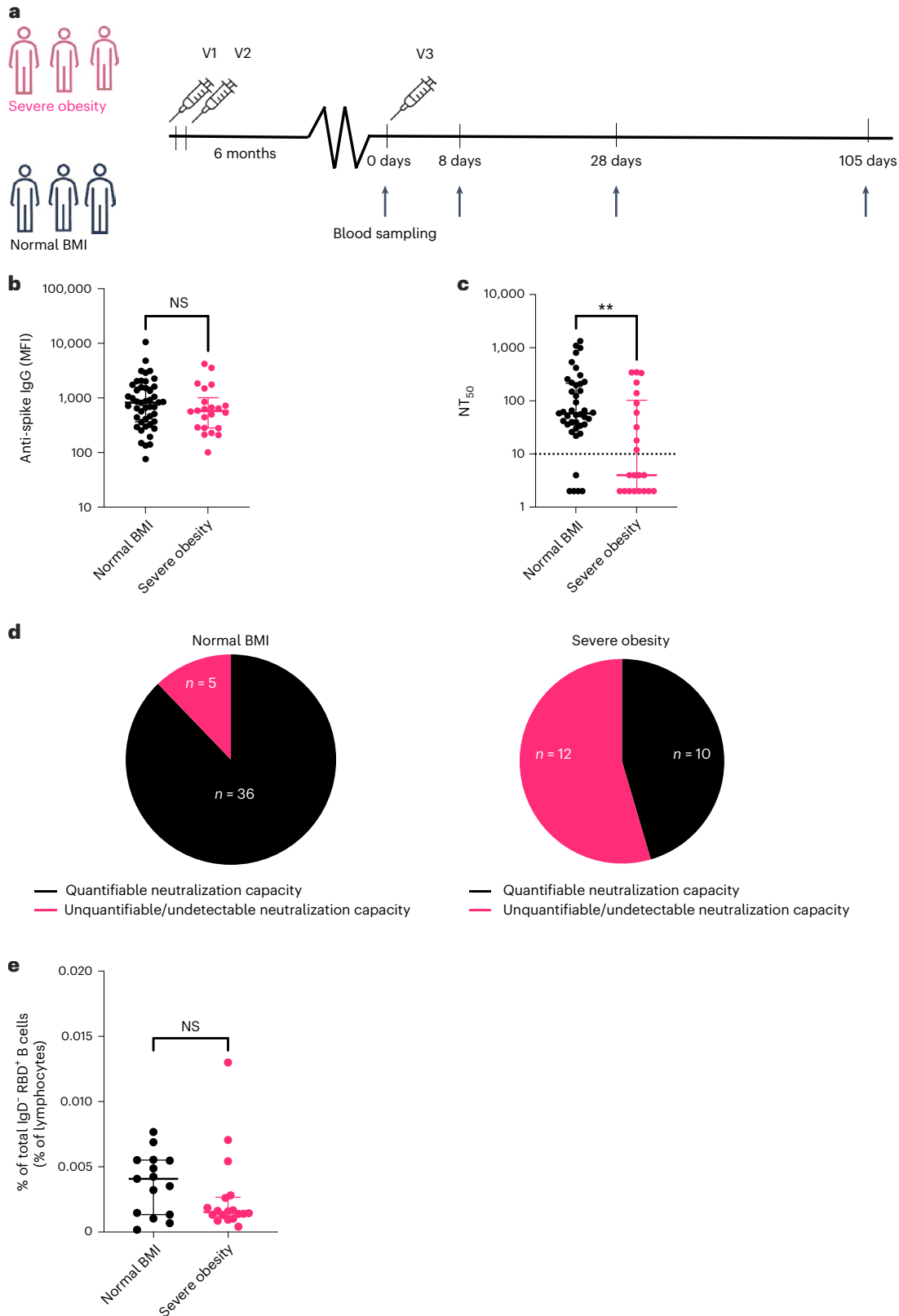
interquartile range. **c**,  $NT_{50}$  against wild-type SARS-CoV-2, with the dotted line indicating the limit of quantification. Horizontal bars indicate the median and interquartile range. **\*\*** $P = 0.061$  in two-sided Mann–Whitney test. **d**, Proportion of individuals in both groups with unquantifiable or undetectable versus quantifiable titers of neutralizing antibodies. **e**, Frequency of antigen-experienced (IgD<sup>+</sup>) RBD-binding (RBD<sup>+</sup>) B cells 6 months after the primary vaccination course. Data are expressed as a percentage (%) of the total number of lymphocytes in individuals with severe obesity ( $n = 18$ , magenta) and individuals with normal weight ( $n = 15$ , black). Horizontal bars indicate the median and interquartile range.  $P$  values are from Mann–Whitney  $U$ -tests. NS, not significant.



accelerated in individuals with severe obesity. Furthermore, we demonstrate that severe obesity does not lead to a failure to target neutralizing spike epitopes. Rather, the relative reduction in neutralizing capacity may result from a lack of high-affinity antibodies. Indeed, our findings are similar to those seen in individuals with obesity after influenza vaccination, with no difference in early immunogenicity but quicker waning associated with higher risk of influenza or influenza-like illness

in individuals with obesity throughout the influenza season<sup>37</sup>. Further studies will be needed to test whether hyperglycemia modifies the risk associated with severe obesity.

Limitations of the current study include the definition of severe COVID-19 outcomes in the EAVE II population study, which may include individuals who were hospitalized for other reasons but in whom infection was incidentally detected. This definition likely affects individuals



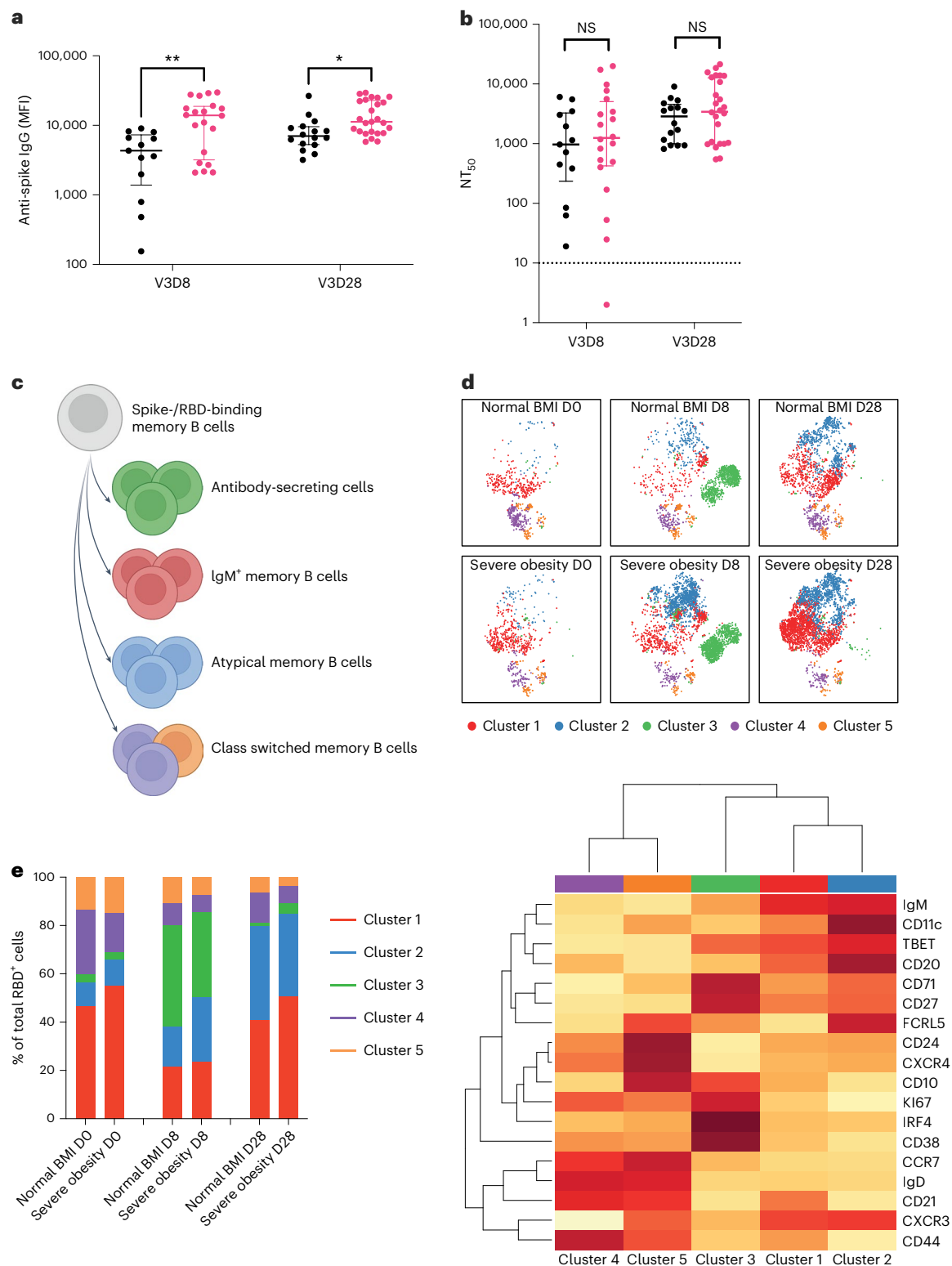


**Fig. 3 | Immune response to third (booster) dose COVID-19 vaccination.** Individuals with severe obesity ( $n = 25$ , magenta) and normal BMI controls ( $n = 16$ , black) were studied at day 8 (D8) and day 28 (D28) after the third vaccine dose (V3). **a**, Levels of anti-spike IgG antibodies (MFI) at day 8 (\*\* $P = 0.0024$ , mixed-effects analysis with Sidak's multiple comparisons tests) and day 28 (\* $P = 0.0199$ , mixed-effects analysis with Sidak's multiple comparisons tests). Horizontal bars indicate the median and interquartile range. **b**, NT<sub>50</sub> against wild-type SARS-CoV-2 at days 8 and 28, with the dotted line indicating the limit of quantification. Horizontal bars indicate the median and interquartile range.

**c**, Schematic depicting the differentiation of B cells in response to vaccine administration. **d**, High-dimensional spectral flow cytometry of SARS-CoV-2 RBD-binding B cells. tSNE and FlowSOM analyses of multi-parameter flow cytometry of CD19<sup>+</sup> RBD-binding B cells from individuals with normal weight and individuals with severe obesity before (V3D0), 8 d after (V3D8) and 28 d after (V3D28) a booster mRNA vaccine (top panel). Bottom panel: heat map of row-normalized mean protein expression on different clusters of cells; red indicates high expression, and yellow indicates low expression. **e**, Frequency of RBD-binding B cells between groups over time. NS, not significant.

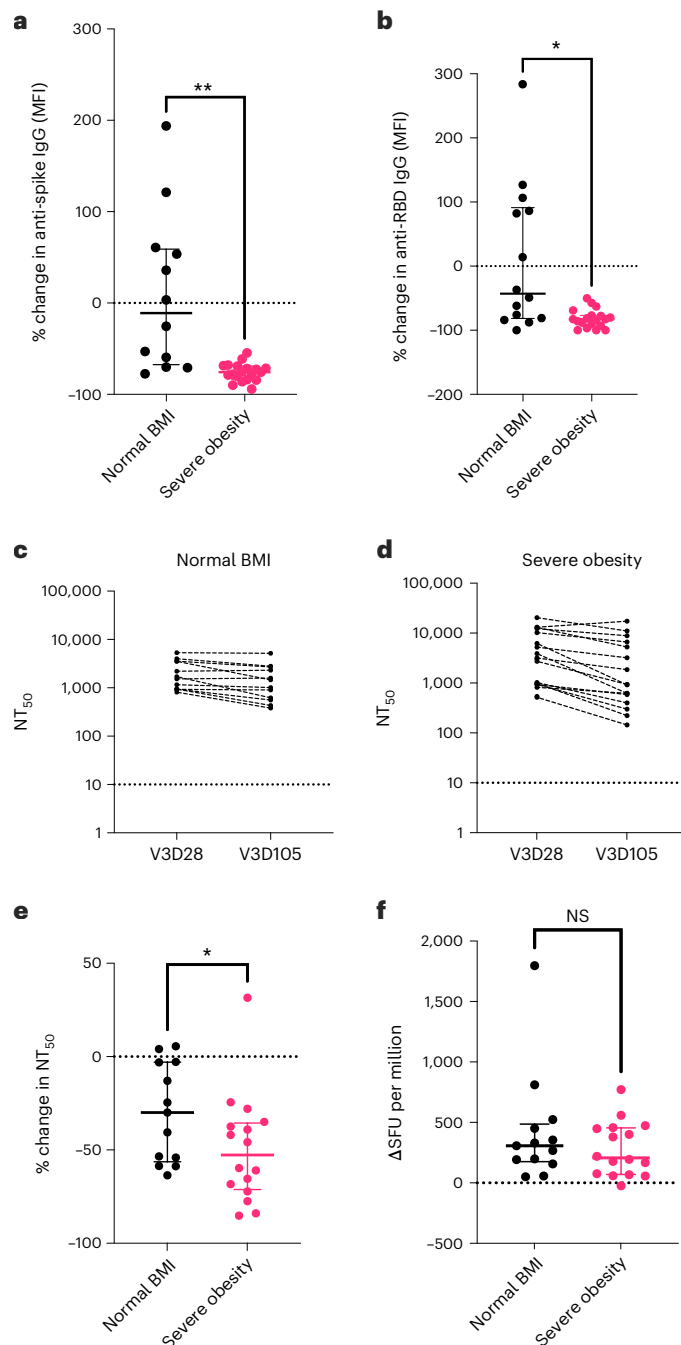


**Fig. 4 | Third-dose COVID-19 vaccine-induced immunity in individuals with severe obesity.** Individuals with severe obesity ( $n = 19$ , magenta) and normal BMI controls ( $n = 14$ , black) were studied at day 28 and day 105 after the third vaccine dose. **a**, Percentage (%) change in anti-spike IgG antibody levels (MFI). Horizontal bars indicate the median and interquartile range (\*\* $P = 0.0057$  in Welch's  $t$ -test). **b**, Percentage (%) change in anti-RBD IgG antibody levels between these two timepoints. Horizontal bars indicate the median and interquartile range (\* $P = 0.0102$  in Welch's  $t$ -test). **c, d**,  $NT_{50}$  measured at 28 d (V3D28) and 105 d (V3D105) after third-dose vaccination (V3) in normal BMI controls (**c**) and individuals with severe obesity (**d**). **e**, Percentage (%) change in  $NT_{50}$  against wild-type SARS-CoV-2, with the dotted line indicating the limit of quantification. Horizontal bars indicate the median and interquartile range (\* $P = 0.0448$  in Mann-Whitney test). Dotted line indicates no change. **f**, T cell responses quantified by ELISpot. Horizontal bars indicate the median and interquartile range. Individuals who reported a positive SARS-CoV-2 RT-PCR test between day 28 and day 105 or who had positive anti-nucleocapsid antibodies at day 105 were excluded from these analyses. NS, not significant.

in all BMI categories similarly (post hoc sensitivity analysis in clinically confirmed cases generated very similar results). BMI data were collected only once in EAVE II, and, thus, we cannot account for changes in BMI over time. However, there is substantial evidence that the secular trend is for BMI to increase over time, which means that any bias is likely to operate differentially toward the null (some individuals classified as having normal BMI might have obesity). Any misclassification error is, therefore, likely to underestimate associations between high BMI and severe COVID-19 outcomes. The number of individuals studied in the SCORPIO study was relatively modest and means that there is a risk of type II errors. Due to sample size, it is not feasible to perform a multivariate analysis to account for other variables, which could potentially affect immunogenicity. Additionally, our study is underpowered to directly test whether there is an association between type 2 diabetes and/or drugs prescribed for metabolic disease and specific immuno-phenotypes.

There is substantial evidence that weight loss of at least 5% can reduce the risk of type 2 diabetes and other metabolic complications. Accordingly, it is likely that lifestyle modification, pharmacotherapy and bariatric surgery—interventions that can lead to a reduction in body weight and improvement in metabolic health—could similarly ameliorate COVID-19 outcomes. Further studies in individuals in the weight-reduced state will be important to establish whether weight loss can mediate beneficial effects on humoral immunity and, thus, offer improved protection against COVID-19 in both vaccinated and unvaccinated individuals. We conclude that individuals with obesity show a reduction in the maintenance of humoral vaccine responses, and we suggest that additional or more frequent booster doses are likely to be required to maintain protection against COVID-19. Due to the high prevalence of obesity<sup>38</sup>, this poses a major challenge for health services and vaccine programs around the world.

## Online content

Any methods, additional references, Nature Portfolio reporting summaries, source data, extended data, supplementary information, acknowledgements, peer review information; details of author contributions and competing interests; and statements of data and code availability are available at <https://doi.org/10.1038/s41591-023-02343-2>.

## References

- Popkin, B. M. et al. Individuals with obesity and COVID-19: a global perspective on the epidemiology and biological relationships. *Obes. Rev.* **21**, e13128 (2020).
- Gao, M. et al. Associations between body-mass index and COVID-19 severity in 6.9 million people in England: a prospective, community-based, cohort study. *Lancet Diabetes Endocrinol.* **9**, 350–359 (2021).
- Arbel, R. et al. BNT162b2 vaccine booster and mortality due to Covid-19. *N. Engl. J. Med.* **385**, 2413–2420 (2021).
- Barron, E. et al. Associations of type 1 and type 2 diabetes with COVID-19-related mortality in England: a whole-population study. *Lancet Diabetes Endocrinol.* **8**, 813–822 (2020).
- Grasselli, G. et al. Baseline characteristics and outcomes of 1591 patients infected with SARS-CoV-2 admitted to ICUs of the Lombardy Region, Italy. *JAMA* **323**, 1574–1581 (2020).
- Dashtban, A. et al. A retrospective cohort study predicting and validating impact of the COVID-19 pandemic in individuals with chronic kidney disease. *Kidney Int.* **102**, 652–660 (2022).
- Alvarez-Garcia, J. et al. Prognostic impact of prior heart failure in patients hospitalized with COVID-19. *J. Am. Coll. Cardiol.* **76**, 2334–2348 (2020).
- Polack, F. P. et al. Safety and efficacy of the BNT162b2 mRNA Covid-19 vaccine. *N. Engl. J. Med.* **383**, 2603–2615 (2020).
- Baden, L. R. et al. Efficacy and safety of the mRNA-1273 SARS-CoV-2 vaccine. *N. Engl. J. Med.* **384**, 403–416 (2021).

10. Khoury, D. S. et al. Neutralizing antibody levels are highly predictive of immune protection from symptomatic SARS-CoV-2 infection. *Nat. Med.* **27**, 1205–1211 (2021).
11. Edara, V. V. et al. Infection and vaccine-induced neutralizing antibody responses to the SARS-CoV-2 B.1.617.1 variant. *N. Engl. J. Med.* **385**, 664–666 (2021).
12. Gilbert, P. B. et al. Immune correlates analysis of the mRNA-1273 COVID-19 vaccine efficacy clinical trial. *Science* **375**, 43–50 (2022).
13. Katikireddi, S. V. et al. Two-dose ChAdOx1 nCoV-19 vaccine protection against COVID-19 hospital admissions and deaths over time: a retrospective, population-based cohort study in Scotland and Brazil. *Lancet* **399**, 25–35 (2022).
14. Goldberg, Y. et al. Waning immunity after the BNT162b2 vaccine in Israel. *N. Engl. J. Med.* **385**, e85 (2021).
15. Eliakim, A., Schwindt, C., Zaldivar, F., Casali, P. & Cooper, D. M. Reduced tetanus antibody titers in overweight children. *Autoimmunity* **39**, 137–141 (2006).
16. Painter, S. D., Ovsyannikova, I. G. & Poland, G. A. The weight of obesity on the human immune response to vaccination. *Vaccine* **33**, 4422–4429 (2015).
17. Sheridan, P. A. et al. Obesity is associated with impaired immune response to influenza vaccination in humans. *Int. J. Obes. (Lond.)* **36**, 1072–1077 (2012).
18. Banga, N., Guss, P., Banga, A. & Rosenman, K. D. Incidence and variables associated with inadequate antibody titers after pre-exposure rabies vaccination among veterinary medical students. *Vaccine* **32**, 979–983 (2014).
19. Levin, E. G. et al. Waning immune humoral response to BNT162b2 Covid-19 vaccine over 6 months. *N. Engl. J. Med.* **385**, e84 (2021).
20. Herzberg, J. et al. Persistence of immune response in health care workers after two doses BNT162b2 in a longitudinal observational study. *Front. Immunol.* **13**, 839922 (2022).
21. Yamamoto, S. et al. Sex-associated differences between BMI and SARS-CoV-2 antibody titers following the BNT162b2 vaccine. *Obes. (Silver Spring)* **30**, 999–1003 (2022).
22. Papadopoulos, D. et al. Predictive factors for neutralizing antibody levels nine months after full vaccination with BNT162b2: results of a machine learning analysis. *Biomedicines* **10**, 204 (2022).
23. Ward, H. et al. Population antibody responses following COVID-19 vaccination in 212,102 individuals. *Nat. Commun.* **13**, 907 (2022).
24. Mallow, C. et al. Real world SARS-COV-2 vaccine effectiveness in a Miami academic institution. *Am. J. Emerg. Med.* **54**, 97–101 (2022).
25. Chhabria, S. & Stanford, F. C. A long shot: the importance of needle length in vaccinating patients with obesity against COVID-19. *Vaccine* **40**, 9–10 (2022).
26. Mulholland, R. H. et al. Cohort profile: Early Pandemic Evaluation and Enhanced Surveillance of COVID-19 (EAVE II) database. *Int. J. Epidemiol.* **50**, 1064–1074 (2021).
27. Agrawal, U. et al. COVID-19 hospital admissions and deaths after BNT162b2 and ChAdOx1 nCoV-19 vaccinations in 2.57 million people in Scotland (EAVE II): a prospective cohort study. *Lancet Respir. Med.* **9**, 1439–1449 (2021).
28. Simpson, C. R. et al. Early Pandemic Evaluation and Enhanced Surveillance of COVID-19 (EAVE II): protocol for an observational study using linked Scottish national data. *BMJ Open* **10**, e039097 (2020).
29. Vasileiou, E. et al. Investigating the uptake, effectiveness and safety of COVID-19 vaccines: protocol for an observational study using linked UK national data. *BMJ Open* **12**, e050062 (2022).
30. Gerber, P. P. et al. A protease-activatable luminescent biosensor and reporter cell line for authentic SARS-CoV-2 infection. *PLoS Pathog.* **18**, e1010265 (2022).
31. Burton, A. R. et al. The memory B cell response to influenza vaccination is impaired in older persons. *Cell Rep.* **41**, 111613 (2022).
32. Cancro, M. P. Age-associated B cells. *Annu. Rev. Immunol.* **38**, 315–340 (2020).
33. Hill, D. L. et al. The adjuvant GLA-SE promotes human Tfh cell expansion and emergence of public TCRβ clonotypes. *J. Exp. Med.* **216**, 1857–1873 (2019).
34. Garcia-Beltran, W. F. et al. COVID-19-neutralizing antibodies predict disease severity and survival. *Cell* **184**, 476–488 (2021).
35. Rees-Spear, C. et al. The effect of spike mutations on SARS-CoV-2 neutralization. *Cell Rep.* **34**, 108890 (2021).
36. Bergwerk, M. et al. Covid-19 breakthrough infections in vaccinated health care workers. *N. Engl. J. Med.* **385**, 1474–1484 (2021).
37. Neidich, S. D. et al. Increased risk of influenza among vaccinated adults who are obese. *Int. J. Obes. (Lond.)* **41**, 1324–1330 (2017).
38. Ward, Z. J. et al. Projected U.S. state-level prevalence of adult obesity and severe obesity. *N. Engl. J. Med.* **381**, 2440–2450 (2019).

**Publisher's note** Springer Nature remains neutral with regard to jurisdictional claims in published maps and institutional affiliations.

**Open Access** This article is licensed under a Creative Commons Attribution 4.0 International License, which permits use, sharing, adaptation, distribution and reproduction in any medium or format, as long as you give appropriate credit to the original author(s) and the source, provide a link to the Creative Commons license, and indicate if changes were made. The images or other third party material in this article are included in the article's Creative Commons license, unless indicated otherwise in a credit line to the material. If material is not included in the article's Creative Commons license and your intended use is not permitted by statutory regulation or exceeds the permitted use, you will need to obtain permission directly from the copyright holder. To view a copy of this license, visit <http://creativecommons.org/licenses/by/4.0/>.

© The Author(s) 2023

**Agatha A. van der Klaauw** <sup>1</sup>, **Emily C. Horner** <sup>2,25</sup>, **Pehuén Pereyra-Gerber** <sup>3,4,25</sup>, **Utkarsh Agrawal** <sup>5,25</sup>, **William S. Foster** <sup>6</sup>, **Sarah Spencer**<sup>2</sup>, **Bensi Vergese**<sup>1,7</sup>, **Miriam Smith**<sup>1</sup>, **Elana Henning**<sup>1</sup>, **Isobel D. Ramsay** <sup>3,4,8</sup>, **Jack A. Smith** <sup>3,4</sup>, **Stephane M. Guillaume** <sup>6</sup>, **Hayley J. Sharpe** <sup>6</sup>, **Iain M. Hay** <sup>6,9</sup>, **Sam Thompson**<sup>6</sup>, **Silvia Innocentin**<sup>6</sup>, **Lucy H. Booth**<sup>2</sup>, **Chris Robertson**<sup>10</sup>, **Colin McCowan** <sup>5</sup>, **Steven Kerr**<sup>11</sup>, **Thomas E. Mulrone**<sup>2</sup>, **Martin J. O'Reilly** <sup>2</sup>, **Thevinya P. Gurugama**<sup>2</sup>, **Lihinya P. Gurugama**<sup>2</sup>, **Maria A. Rust**<sup>2</sup>, **Alex Ferreira** <sup>2</sup>, **Soraya Ebrahimi**<sup>12,13</sup>, **Lourdes Ceron-Gutierrez**<sup>12,13</sup>, **Jacopo Scotucci**<sup>1</sup>, **Barbara Kronsteiner** <sup>14</sup>, **Susanna J. Dunachie** <sup>14,15,16,17,18</sup>, **Paul Klenerman** <sup>14,15,16,17</sup>, **PITCH Consortium**<sup>\*</sup>, **Adrian J. Park** <sup>13</sup>, **Francesco Rubino**<sup>19</sup>, **Abigail A. Lamikanra**<sup>20,21</sup>, **Hannah Stark**<sup>22</sup>, **Nathalie Kingston**<sup>22</sup>, **Lise Estcourt**<sup>20,21</sup>, **Heli Harvala**<sup>23</sup>, **David J. Roberts**<sup>20,21</sup>, **Rainer Doffinger**<sup>12,13</sup>, **Michelle A. Linterman** <sup>6</sup>, **Nicholas J. Matheson** <sup>3,4,8,24,25</sup>, **Aziz Sheikh** <sup>11,25</sup> ✉, **I. Sadaf Farooqi** <sup>1,25</sup> ✉ & **James E. D. Thaventhiran** <sup>2,25</sup> ✉



<sup>1</sup>University of Cambridge Metabolic Research Laboratories and NIHR Cambridge Biomedical Research Centre, Wellcome-Medical Research Council (MRC) Institute of Metabolic Science, University of Cambridge, Cambridge, UK. <sup>2</sup>MRC Toxicology Unit, University of Cambridge, Cambridge, UK. <sup>3</sup>Cambridge Institute of Therapeutic Immunology and Infectious Disease, University of Cambridge, Cambridge, UK. <sup>4</sup>Department of Medicine, University of Cambridge, Cambridge, UK. <sup>5</sup>Nuffield Department of Primary Care Health Sciences, University of Oxford, Oxford, UK. <sup>6</sup>Babraham Institute, Babraham Research Campus, Cambridge, UK. <sup>7</sup>NIHR Cambridge Clinical Research Facility, Cambridge University Hospitals NHS Foundation Trust, Cambridge, UK. <sup>8</sup>Department of Infectious Diseases, Cambridge University Hospitals NHS Foundation Trust, Cambridge, UK. <sup>9</sup>Cambridge Institute for Medical Research, University of Cambridge, Cambridge, UK. <sup>10</sup>Department of Mathematics and Statistics, University of Strathclyde, Glasgow, UK. <sup>11</sup>Usher Institute, University of Edinburgh, Edinburgh, UK. <sup>12</sup>Immunology, Cambridge University Hospitals NHS Foundation Trust, Cambridge, UK. <sup>13</sup>Clinical Biochemistry, Cambridge University Hospitals NHS Foundation Trust, Cambridge, UK. <sup>14</sup>Peter Medawar Building for Pathogen Research, Nuffield Department of Clinical Medicine, University of Oxford, Oxford, UK. <sup>15</sup>NDM Centre for Global Health Research, Nuffield Department of Medicine, University of Oxford, Oxford, UK. <sup>16</sup>NIHR Oxford Biomedical Research Centre, Oxford University Hospitals NHS Foundation Trust, Oxford, UK. <sup>17</sup>Translational Gastroenterology Unit, University of Oxford, Oxford, UK. <sup>18</sup>Mahidol-Oxford Tropical Medicine Research Unit, Bangkok, Thailand. <sup>19</sup>Department of Diabetes, King's College London and King's College Hospital NHS Foundation Trust, London, UK. <sup>20</sup>NHS Blood and Transplant, Oxford, UK. <sup>21</sup>Radcliffe Department of Medicine, University of Oxford, Oxford, UK. <sup>22</sup>NIHR BioResource, Cambridge University Hospitals NHS Foundation Trust, Cambridge, UK. <sup>23</sup>NHS Blood and Transplant, London, UK. <sup>24</sup>NHS Blood and Transplant, Cambridge, UK. <sup>25</sup>These authors contributed equally: Emily C. Horner, Pehuén Pereyra-Gerber, Utkarsh Agrawal, Nicholas J. Matheson, Aziz Sheikh, I. Sadaf Farooqi, James E. D. Thaventhiran. \*A full list of members and their affiliations appears in the Supplementary Data Table 10. ✉e-mail: [aziz.sheikh@ed.ac.uk](mailto:aziz.sheikh@ed.ac.uk); [isf20@cam.ac.uk](mailto:isf20@cam.ac.uk); [jedt2@cam.ac.uk](mailto:jedt2@cam.ac.uk)

## Methods

### EAVE II study

The EAVE II surveillance platform drew on near-real-time nationwide healthcare data for 5.4 million individuals (~99%) in Scotland<sup>26–29</sup>. It includes information on clinical and demographic characteristics of each individual, their vaccination status and type of vaccine used and information on positive SARS-CoV-2 infection and subsequent hospitalization or death. Ethical approval was granted by the National Research Ethics Service Committee, Southeast Scotland 02 (reference 12/SS/0201) for the study using the EAVE II platform. Approval for data linkage was granted by the Public Benefit and Privacy Panel for Health and Social Care (reference 1920-0279). Individual written patient consent was not required for this analysis.

Using data from the EAVE II platform, we examined the impact of obesity (using BMI measurements) and clinical and demographic characteristics, including time since receiving the second and third vaccine doses, previous history of testing positive for COVID-19, gap between vaccine doses and dominant variant in the background, of fully vaccinated adults in Scotland who experienced severe COVID-19 outcomes. The cohort analyzed for this study consisted of individuals aged 18 years and older who were administered with at least two doses of BNT162b2 mRNA, ChAdOx1 nCoV-19 or mRNA-1273 vaccines between 8 December 2020 and 19 March 2022. Follow-up began 14 d after receiving the second dose until COVID-19-related hospitalization, COVID-19-related death or the end of study period (that is, 19 March 2022). All the COVID-19-related hospital admissions or deaths were selected between 14 September 2021 and 19 March 2022. We excluded events that occurred within the first 14 d after completing the primary vaccination schedule to allow for time for a full immune response to be mounted. Patients without immunosuppression had their primary vaccination schedule with two doses, and so the third dose is a booster. For people with immunosuppression, the primary vaccination schedule was for three vaccine doses. BMI was available for individuals based on last recorded measurement within their primary care record. Where the BMI was missing, it was imputed using ordinary least squares regression with all QCovid risk groups<sup>39</sup> together with age, sex and deprivation included as predictors. The coding systems used in Scotland are Read for GP data and ICD-10 for hospitalization data. This information is provided in more detail in the EAVE II protocol and cohort profile<sup>39</sup> and data dictionary (<https://www.ed.ac.uk/usher/eave-ii>) and at <https://github.com/EAVE-II/EAVE-II-data-dictionary>.

**Definition of outcomes.** The primary outcome of interest was severe COVID-19, which was defined as COVID-19-related hospital admission or death 14 d or more after receiving the second vaccine or booster dose<sup>40</sup>. COVID-19-related hospital admission was defined as hospital admission within 14 d of a positive RT-PCR test or COVID-19 as reason for admission or a positive SARS-CoV-2 RT-PCR test result during an admission where COVID-19 was not the reason for admission. COVID-19-related mortality was defined as either death for any reason within 28 d of a positive RT-PCR test or where COVID-19 was recorded as the primary reason for death on the death certificate.

**Population characteristics and confounders.** Characteristics of interest were defined at baseline on 8 December 2020 and included age, sex, socioeconomic status based on quintiles of the SIMD, urban or rural place of residence (which is a measure of rurality based on residential settlement), BMI, previous natural infection from SARS-CoV-2 before second dose of the vaccine (classified as 0–3 months, 3–6 months, 6–9 months and  $\geq 9$  months before second vaccine dose), number of pre-existing comorbidities known to be linked with severe COVID-19 outcome and being in a high-risk occupational group, defined as someone with undergoing regular RT-PCR testing<sup>27</sup>. Time since vaccination was distributed in the periods of 3–10 weeks, 11–15 weeks, 16–20 weeks and  $\geq 21$  weeks from completion of second dose of the

primary vaccination and 3–5 weeks, 6–8 weeks and  $\geq 9$  weeks for the booster doses separately. To allow for variation in background levels of community infection, we split the data by calendar week. BMI was grouped as  $<18.5$  kg/m<sup>2</sup> (underweight), 18.5–24.9 kg/m<sup>2</sup> (normal weight), 25–29.9 kg/m<sup>2</sup> (overweight), 30–39.9 kg/m<sup>2</sup> (obese) and  $\geq 40$  kg/m<sup>2</sup> (severely obese) according to World Health Organization (WHO) criteria.

**EAVE II statistical analysis.** We calculated the frequency and rate per 1,000 person-years of severe COVID-19 outcomes for all demographic and clinical factors. Generalized linear models (GLMs) assuming a Poisson distribution with person-time as an offset representing the time at risk were used to derive rate ratios (RRs) with 95% CIs for the association between demographic and clinical factors and COVID-19-related hospitalization or death. aRRs were estimated adjusting for all confounders, including age, sex, SIMD, time since receiving the second dose of vaccine, pre-existing comorbidities, the gap between vaccine doses, previous history of SARS-CoV-2 infection and calendar time. SIMD looks at the extent to which an area is deprived across seven domains: income, employment, education, health, access to services, crime and housing. SIMD was allocated based on an individual's home postcode, with quintiles of population ranging from 1 for the most deprived 20% to 5 for the least deprived 20% of the population.

We conducted a post hoc sensitivity analysis in clinically confirmed cases. Because BMI was not available for all the individuals, missing BMI was imputed using ordinary least squares regression with all other independent variables included as predictors. We conducted a post hoc sensitivity analysis by imputing the missing BMI using an average of 10 least squares regressions (multiple imputation). R (version 3.6.1) was used to carry out all statistical analyses.

### Ethical approval and study populations

**SCORPIO clinical study.** Clinical studies in individuals with severe obesity and normal BMI controls were approved by the National Research Ethics Committee and the Health Research Authority (East of England–Cambridge Research Ethics Committee (SCORPIO study amendment of 'NIHR BioResource' 17/EE/0025)). Human tonsil samples were collected under ethical approval from the UK Health Research Authority (reference 16/LO/0453). Each participant provided written informed consent. All studies were conducted in accordance with the Declaration of Helsinki and the guidelines for Good Clinical Practice.

Individuals with severe obesity (class II/III WHO criteria of BMI  $\geq 40$  kg/m<sup>2</sup> or BMI  $\geq 35$  kg/m<sup>2</sup> with obesity-associated medical conditions, such as type 2 diabetes and hypertension) who attended the obesity clinic at Cambridge University Hospitals NHS Trust and had received two doses of COVID-19 vaccination (first and second doses of ChAdOx1 nCoV-19 or BNT162b2 mRNA) between December 2021 and May 2022 were invited to take part. Individuals with acquired (HIV, immunosuppressant drugs) or congenital immune deficiencies and cancer were excluded. Third-dose vaccinations (BNT162b2, Pfizer BioNTech or half-dose mRNA1273 (Moderna)) were administered as part of the NHS vaccination program. UK Health Security Agency policy recommends the use of longer needles (38 mm versus 25 mm) in individuals with severe obesity.

Additional normal BMI controls were recruited in Oxford, UK, as part of the PITCH study under the GI Biobank Study 16/YH/0247, approved by the Yorkshire & Humber Sheffield Research Ethics Committee, which was amended for this purpose on 8 June 2020. Samples obtained 6 months after the primary course were included.

Clinical and immunological measurements were taken before the booster vaccination and 8 d ( $-3$ ), 28 d ( $\pm 7$ ) and 105 d ( $\pm 7$ ) after vaccination. Third-dose vaccinations were administered as part of the NHS vaccination program and were mRNA vaccines (BNT162b2 or mRNA1273 (Moderna)). Clinical data regarding comorbidities associated with obesity were obtained from the medical records. Supplementary

Data Table 8 details the demographic characteristics of this cohort. Healthy healthcare workers were enrolled into the longitudinal OPTIC cohort in Oxford, UK, between May 2020 and May 2021 as part of the PITCH consortium. PITCH participants were sampled between July and November 2021, a median of 185 d (range, 155–223) after receiving a second vaccination with ChAdOX1 nCoV-19 or BNT162b2 mRNA vaccine. All PITCH participants were classified as infection-naïve, as defined by never having received a positive lateral flow or PCR test for SARS-CoV-2 and negative anti-nucleocapsid antibodies at the time of their first vaccination. Therefore, a total of 28 individuals with severe obesity and 41 normal BMI controls were evaluated 6 months after the primary course of vaccination, whereas, for the response to third-dose vaccination, 16 normal BMI controls were studied.

Of the 28 recruited individuals with severe obesity, two had positive anti-nucleocapsid antibodies and reported a positive RT-PCR test before their third-dose vaccination. They were excluded from further analysis. In addition, between day 28 and day 105, two individuals with severe obesity reported positive SARS-CoV-2-tests (lateral flow test or RT-PCR tests as per UK guidelines at the time). They were excluded from the day 28 to day 105 analysis. An additional three people with severe obesity were recruited after they had had their booster for day 28 and day 105 analysis only. In addition, one of the normal-weight individuals had positive anti-nucleocapsid antibodies who had not had a PCR test, before their third-dose vaccination. This individual was excluded from the before and after third-dose analysis. In addition, between day 28 and day 105, two normal-weight individuals reported positive SARS-CoV-2-tests (lateral flow test or PCR tests as per UK guidelines at the time, one of those individuals on two separate occasions). They were excluded from the day 28 to day 105 analysis. Missing data in addition to this were due to (1) occasional difficult venepuncture in individuals with obesity; (2) insufficient peripheral blood mononuclear cells (PBMCs) isolated for both T and B cell analysis; or (3) insufficient sample to run both wild-type and Omicron neutralization assays. Therefore, we specified how many individuals were included per analysis, per figure.

Peripheral blood samples were acquired in either lithium heparin (PBMCs) or serum-separating tubes. Serum tubes were centrifuged at 1,600g for 10 min at room temperature to separate serum from the cell pellet before being aliquoted and stored at  $-80^{\circ}\text{C}$  until use. PBMCs were isolated by layering over Lymphoprep density gradient medium (STEMCELL Technologies), followed by density gradient centrifugation at 800g for 20 min at room temperature. PBMCs were isolated and washed twice using wash buffer ( $1\times$  PBS, 1% FCS, 2 mM EDTA) at 400g for 10 min at  $4^{\circ}\text{C}$ . Isolated PBMCs were resuspended in freezing media, aliquoted and stored at  $-80^{\circ}\text{C}$  for up to 1 week before being transferred to liquid nitrogen until use.

#### **SARS-CoV-2 serology by multiplex particle-based flow cytometry.**

Recombinant SARS-CoV-2 nucleocapsid, spike and RBD were covalently coupled to distinct bead sets (Luminex) to form a three-plex and analyzed as previously described<sup>41</sup>. Specific binding was reported as mean fluorescence intensity (MFI).

**Neutralizing antibodies to SARS-CoV-2.** Luminescent HEK293T-ACE2-30F-PLP2 reporter cells (clone B7) expressing ACE2 and SARS-CoV-2 papain-like protease-activatable circularly permuted firefly luciferase (FFluc) are available from the National Institute for Biological Standards and Control (NIBSC, <https://www.nibsc.org/>, cat. no. 101062)<sup>30</sup>. They were cultured in IMDM supplemented with 4 mM GlutaMAX (Gibco), 10% FCS, 100 U ml<sup>-1</sup> penicillin and 0.1 mg ml<sup>-1</sup> streptomycin at  $37^{\circ}\text{C}$  in 5% CO<sub>2</sub>, regularly screened and confirmed to be mycoplasma negative (Lonza MycoAlert).

The SARS-CoV-2 viruses used in this study were a wild-type (lineage B) isolate (SARS-CoV-2/human/Liverpool/REMRQ0001/2020), a kind gift from Ian Goodfellow (University of Cambridge), isolated by Lance

Turtle (University of Liverpool), David Matthews and Andrew Davidson (University of Bristol)<sup>42,43</sup>, and an Omicron (lineage B.1.1.529) variant, a kind gift from Ravindra Gupta<sup>44</sup>. Unless otherwise indicated, all data shown refer to neutralization of wild-type virus.

Sera were heat inactivated at  $56^{\circ}\text{C}$  for 30 min before use, and NT<sub>50</sub> values were measured as previously described<sup>30,45</sup>. In brief, luminescent HEK293T-ACE2-30F-PLP2 reporter cells (clone B7) expressing SARS-CoV-2 papain-like protease-activatable circularly permuted FFluc were seeded in flat-bottomed 96-well plates. The next day, SARS-CoV-2 viral stock (multiplicity of infection (MOI) = 0.01) was pre-incubated with a three-fold dilution series of each serum for 2 h at  $37^{\circ}\text{C}$  and then added to the cells. Sixteen hours after infection, cells were lysed in Bright-Glo Luciferase Buffer (Promega) diluted 1:1 with PBS and 1% NP-40, and FFluc activity was measured by luminometry.

Experiments were conducted in duplicate. To obtain NT<sub>50</sub> values, titration curves were plotted as FFluc versus log (serum dilution) and then analyzed by nonlinear regression using the Sigmoidal, 4PL, X is log(concentration) function in GraphPad Prism. NT<sub>50</sub> values were reported when (1) at least 50% inhibition was observed at the lowest serum dilution tested (1:10) and (2) a sigmoidal curve with a good fit was generated. For purposes of visualization and ranking, samples with no neutralizing activity were assigned an arbitrary NT<sub>50</sub> value of 2. Samples for which visual inspection of the titration curve indicated inhibition at low dilutions, but that did not meet criteria (1) and (2) above, were assigned an arbitrary NT<sub>50</sub> value of 4.

To confirm the linearity of the assay, a high-titer positive control serum sample was spiked into FCS (serum dilution series), and then each dilution was treated as a separate sample. Expected and obtained NT<sub>50</sub> values against wild-type SARS-CoV-2 were compared by linear regression, generating a coefficient of determination (R<sup>2</sup>) of 1.00 for dilutions above the limit of quantification (Extended Data Fig. 8a,b).

As a measure of intermediate precision<sup>46</sup>, inter-assay variability was quantified for a medium-titer control serum sample tested against wild-type SARS-CoV-2 in 18 independent experiments conducted over a period 18 months by two different laboratory scientists, revealing a coefficient of variation (CV) of 27% (Extended Data Fig. 8c).

For external validation, a panel of 28 serum samples from NHS Blood and Transplant convalescent plasma donors participating in the C-VELVET study (approved by the West Midlands Solihull Research Ethics Committee, reference 21/WM/0082, IRAS project ID 296926) was tested blinded against both wild-type and Omicron variant SARS-CoV-2. NT<sub>50</sub> values were compared with previously reported focus reduction neutralization test (FRNT) results obtained at the University of Oxford<sup>47</sup>, revealing a Spearman's rank correlation coefficient ( $\rho$ ) of 0.9696 (Extended Data Fig. 8d).

Finally, to enable comparison with other studies, the neutralizing capacity of WHO International Standard 20/136 against wild-type SARS-CoV-2 was measured in five independent experiments, yielding a geometric mean NT<sub>50</sub> of 1,967 (Extended Data Fig. 8e,f). This standard comprises pooled convalescent plasma obtained from 11 individuals which, when reconstituted, is assigned an arbitrary neutralizing capacity of 1,000 IU ml<sup>-1</sup> against early 2020 SARS-CoV-2 isolates<sup>48</sup>. NT<sub>50</sub> values against wild-type SARS-CoV-2 from this study may, therefore, be converted to IU ml<sup>-1</sup> using a calibration factor of 1,000/1,967 (0.51), with a limit of quantification of 5.1 IU ml<sup>-1</sup> (corresponding to an NT<sub>50</sub> value of 10).

**T cell cytokine production.** Antigen-specific T cell responses were assessed using an ELISpot assay as previously described<sup>49</sup>. Results are expressed as spot forming units (SFU) per 10<sup>6</sup> PBMCs. Analysis was completed using GraphPad Prism software version 9.3.1. The comparison of means between groups was performed using two-way, mixed-model ANOVA.



**Quantitation of lymphocyte types and subsets by spectral flow cytometry.** Generation of RBD-specific B cell probes and measurement of RBD-specific B cells were measured by high-dimension flow cytometry as described previously<sup>50,51</sup>. In brief, for flow cytometry stains, a single-cell suspension was prepared from cryopreserved PBMC samples as follows. First, 1 ml of PBMC samples was de-frosted in a 37 °C water bath and then immediately diluted into 9 ml of pre-warmed RPMI + 10% FBS. Cells were washed twice with 10 ml of FACS buffer (PBS containing 2% FBS and 1 mM EDTA). Cells were then resuspended in 500 µl of FACS buffer, and cell numbers and viability were determined using a Countess automated cell counter (Invitrogen). Next,  $5 \times 10^6$  viable cells were transferred to 96-well plates for antibody staining (dilutions used are provided in Supplementary Table 9). Cells were then washed once with FACS buffer and stained with 100 µl of surface antibody mix (including B cell probes) for 2 h at 4 °C. Cells were then washed twice with FACS buffer and fixed with the eBioscience Fcγ3/Transcription Factor Staining Buffer (Thermo Fisher Scientific, 00-5323-00) for 30 min at 4 °C. Cells were then washed with 1× eBioscience Fcγ3/Transcription Factor Permeabilization Buffer (Thermo Fisher Scientific, 00-8333-56) twice and stained with intracellular antibody mix in permeabilization buffer at 4 °C overnight. After overnight staining, samples were washed twice with 1× permeabilization buffer and once with FACS buffer and acquired on a Cytex Aurora. Cells for single-color controls were prepared in the same manner as the fully stained samples. Manual gating of flow cytometry data was performed using FlowJo version 10.8 software (Tree Star).

**SCORPIO study statistical analysis.** Analysis was completed using GraphPad Prism software version 9.3.1. The comparison of means or medians between groups was performed using two-sided parametric *t*-tests, non-parametric Mann–Whitney *U*-tests or mixed-model tests when appropriate. tSNE, FlowSOM and heat map analyses were performed using R (version 4.1.2), using code that was previously described<sup>52</sup>.

### Reporting summary

Further information on research design is available in the Nature Portfolio Reporting Summary linked to this article.

### Data availability

The epidemiology study data that support the findings of this study are not publicly available because they are based on de-identified national clinical records. These are, however, available by application via Scotland's National Safe Haven from Public Health Scotland. The data used in this study can be accessed by researchers through NHS Scotland's Public Benefit and Privacy Panel via its Electronic Data Research and Innovation Service. Anonymized data from the SCORPIO study are included in the manuscript; stored samples are available from the corresponding authors upon reasonable request. Source data are provided with this paper.

### Code availability

All code used in the EAVE II study is publicly available at <https://github.com/EAVE-II/covid-obesity-humoral-response>.

### References

39. Simpson, C. R. et al. External validation of the QCovid risk prediction algorithm for risk of COVID-19 hospitalisation and mortality in adults: national validation cohort study in Scotland. *Thorax* **77**, 497–504 (2022).
40. Public Health Scotland. *Public Health Scotland COVID-19 & Winter Statistical Report*. [https://publichealthscotland.scot/media/10853/21-12-15-covid19-winter\\_publication\\_report.pdf](https://publichealthscotland.scot/media/10853/21-12-15-covid19-winter_publication_report.pdf) (2021).
41. Xiong, X. et al. A thermostable, closed SARS-CoV-2 spike protein trimer. *Nat. Struct. Mol. Biol.* **27**, 934–941 (2020).
42. Daly, J. L. et al. Neuropilin-1 is a host factor for SARS-CoV-2 infection. *Science* **370**, 861–865 (2020).
43. Patterson, E. I. et al. Methods of inactivation of SARS-CoV-2 for downstream biological assays. *J. Infect. Dis.* **222**, 1462–1467 (2020).
44. Meng, B. et al. Altered TMPRSS2 usage by SARS-CoV-2 Omicron impacts infectivity and fusogenicity. *Nature* **603**, 706–714 (2022).
45. Bergamaschi, L. et al. Longitudinal analysis reveals that delayed bystander CD8<sup>+</sup> T cell activation and early immune pathology distinguish severe COVID-19 from mild disease. *Immunity* **54**, 1257–1275 (2021).
46. Andreasson, U. et al. A practical guide to immunoassay method validation. *Front. Neurol.* **6**, 179 (2015).
47. Harvala, H. et al. Convalescent plasma donors show enhanced cross-reactive neutralizing antibody response to antigenic variants of SARS-CoV-2 following immunization. *Transfusion* **62**, 1347–1354 (2022).
48. Knezevic, I. et al. WHO International Standard for evaluation of the antibody response to COVID-19 vaccines: call for urgent action by the scientific community. *Lancet Microbe* **3**, e235–e240 (2022).
49. Angyal, A. et al. T-cell and antibody responses to first BNT162b2 vaccine dose in previously infected and SARS-CoV-2-naive UK health-care workers: a multicentre prospective cohort study. *Lancet Microbe* **3**, e21–e31 (2022).
50. Silva-Cayetano, A. et al. A booster dose enhances immunogenicity of the COVID-19 vaccine candidate ChAdOx1 nCoV-19 in aged mice. *Med. (N Y)* **2**, 243–262 (2021).
51. Foster, W. S. et al. Tfh cells and the germinal center are required for memory B cell formation & humoral immunity after ChAdOx1 nCoV-19 vaccination. *Cell Rep. Med.* **3**, 100845 (2022).
52. Pasciuto, E. et al. Microglia require CD4 T cells to complete the fetal-to-adult transition. *Cell* **182**, 625–640 (2020).

### Acknowledgements

This epidemiological study is part of the EAVE II project. EAVE II is funded by the Medical Research Council (MRC) (MC\_PC\_19075) with the support of BREATHE—The Health Data Research Hub for Respiratory Health (MC\_PC\_19004), which is funded through the UK Research and Innovation Industrial Strategy Challenge Fund and delivered through Health Data Research UK. This research is part of the Data and Connectivity National Core Study, led by Health Data Research UK in partnership with the Office for National Statistics and funded by UK Research and Innovation (grant MC\_PC\_20058) and National Core Studies—Immunity. Additional support was provided through Public Health Scotland, the Scottish Government Director-General Health and Social Care and the University of Edinburgh. The original EAVE project was funded by the National Institute for Health Research (NIHR) Health Technology Assessment program (11/46/23). We thank D. Kelly from Albasoft (Inverness, UK) for support with making primary care data available and W. Inglis-Humphrey, V. Hammersley and L. Brook (University of Edinburgh) for their support with project management and administration.

The SCORPIO study was supported by the MRC (MR/W020564/1, a core award to J.E.T.; MC\_UU\_0025/12 and MR/T032413/1, awards to N.J.M.) and the Medical Research Foundation (MRF-057-0002-RG-THAV-C0798). Additional support was provided by NHS Blood and Transplant (WPA15-02 to N.J.M.), the Wellcome Trust (Institutional Strategic Support Fund 204845/Z/16/Z to N.J.M.), Addenbrooke's Charitable Trust (900239 to N.J.M.) and the NIHR Cambridge Biomedical Research Centre and NIHR BioResource.

M.A.L. is supported by the Biotechnology and Biological Sciences Research Council (BBSRC) (BBS/E/B/000C0427 and BBS/E/B/000C0428) and is a Lister Institute Fellow and an EMBO



Young Investigator. I.M.H. is supported by a Cambridge Institute for Medical Research PhD studentship. H.J.S. is supported by a Sir Henry Dale Fellowship, jointly funded by the Wellcome Trust and the Royal Society (109407), and a BBSRC institutional program grant (BBS/E/B/000C0433). I.S.F. is supported by the Wellcome Trust (207462/Z/17/Z), the Botnar Fondation, the Bernard Wolfe Health Neuroscience Endowment and an NIHR Senior Investigator Award. External validation of the assays for neutralizing antibodies to SARS-CoV-2 was funded by the National Institute for Health and Care Research (grant COVID-19-RECPLAS to D.J.R.). The PITCH study was funded by the UK Department of Health and Social Care. S.J.D. is funded by an NIHR Global Research Professorship (NIHR300791). P.K. is an NIHR Senior Investigator and is funded by the Wellcome Trust (WT109965MA) and National Institutes of Health grant U19 AI082630. We thank the staff of the obesity clinic at Cambridge University Hospitals for their support in recruitment of participants to the SCORPIO study. Clinical studies were performed in the Wellcome-MRC Institute of Metabolic Science Translational Research Facility, supported by a Wellcome Major Award (208363/Z/17/Z), and in the Cambridge NIHR Clinical Research Facility. The funding bodies had no role in the design or conduct of the study; in collection, management, analysis or interpretation of the data; in preparation, review or approval of the manuscript; or in the decision to submit the manuscript for publication. The views expressed are those of the authors and not necessarily those of the NIHR, the Department of Health and Social Care or the UK government.

### Author contributions

A.A.v.d.K., J.E.D.T. and I.S.F. designed and led the study. U.A., C.M., C.R. and A.S. performed the analyses in the EAVE II cohort. A.S. is the guarantor of this work. A.A.v.d.K., S.S., M.S., B.V., E.H., J.S., A.J.P., H.S., N.K., F.R. and I.S.F. recruited the SCORPIO cohort, performed clinical studies and/or analyzed clinical data. E.C.H. coordinated laboratory studies, including extraction of lymphocytes from clinical samples and T cell assays, with S.S., L.H.B., T.E.M., M.J.O.R., T.P.G., L.P.G., M.A.R. and A.F; these experiments were overseen by J.E.D.T. N.J.M. provided oversight of studies of neutralizing antibodies with wild-type and Omicron variants; experiments were performed by P.P.G., with I.D.R.

and J.A.S., and A.A.L., L.E., H.H. and D.J.R. provided data and samples for external validation. R.D., S.E. and L.C.G. performed measurements of anti-spike and anti-nucleocapsid antibodies. M.A.L. led experiments of quantification of lymphocyte types and subsets by flow cytometry, including computational analysis (tSNE); these experiments were performed by W.S.F., S.M.G., H.J.S., I.M.H., S.T. and S.I. B.K., S.J.D., P.K. and the PITCH Consortium contributed samples from individuals with normal BMI recruited to the PITCH study. All authors approved the final version of the manuscript.

### Competing interests

A.S. is a member of the Scottish Government's Standing Committee on Pandemic Preparedness and the Risk Stratification Subgroup of the UK Government's New and Emerging Respiratory Virus Threats Advisory Group (NERVTAG). He was a member of AstraZeneca's Thrombotic Thrombocytopenic Task Force. All roles are unremunerated. S.J.D. is a Scientific Advisor to the Scottish Parliament on COVID-19, for which she receives a fee. I.S.F. has consulted for Eli Lilly, Novo Nordisk and Rhythm Pharmaceuticals on weight loss drugs. All other authors have no conflicts of interest to declare.

### Additional information

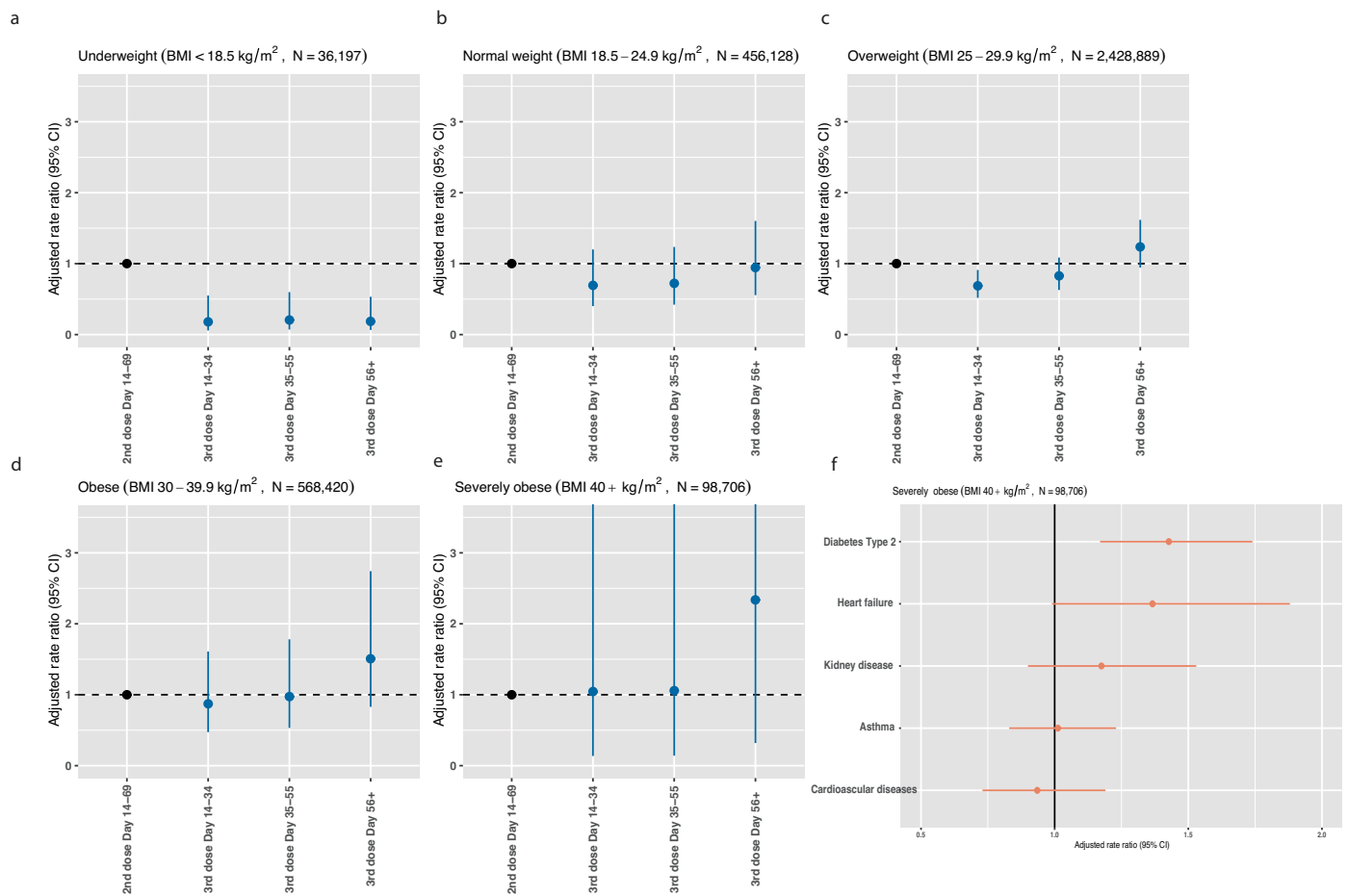
**Extended data** is available for this paper at <https://doi.org/10.1038/s41591-023-02343-2>.

**Supplementary information** The online version contains supplementary material available at <https://doi.org/10.1038/s41591-023-02343-2>.

**Correspondence and requests for materials** should be addressed to Aziz Sheikh, I. Sadaf Farooqi or James E. D. Thaventhiran.

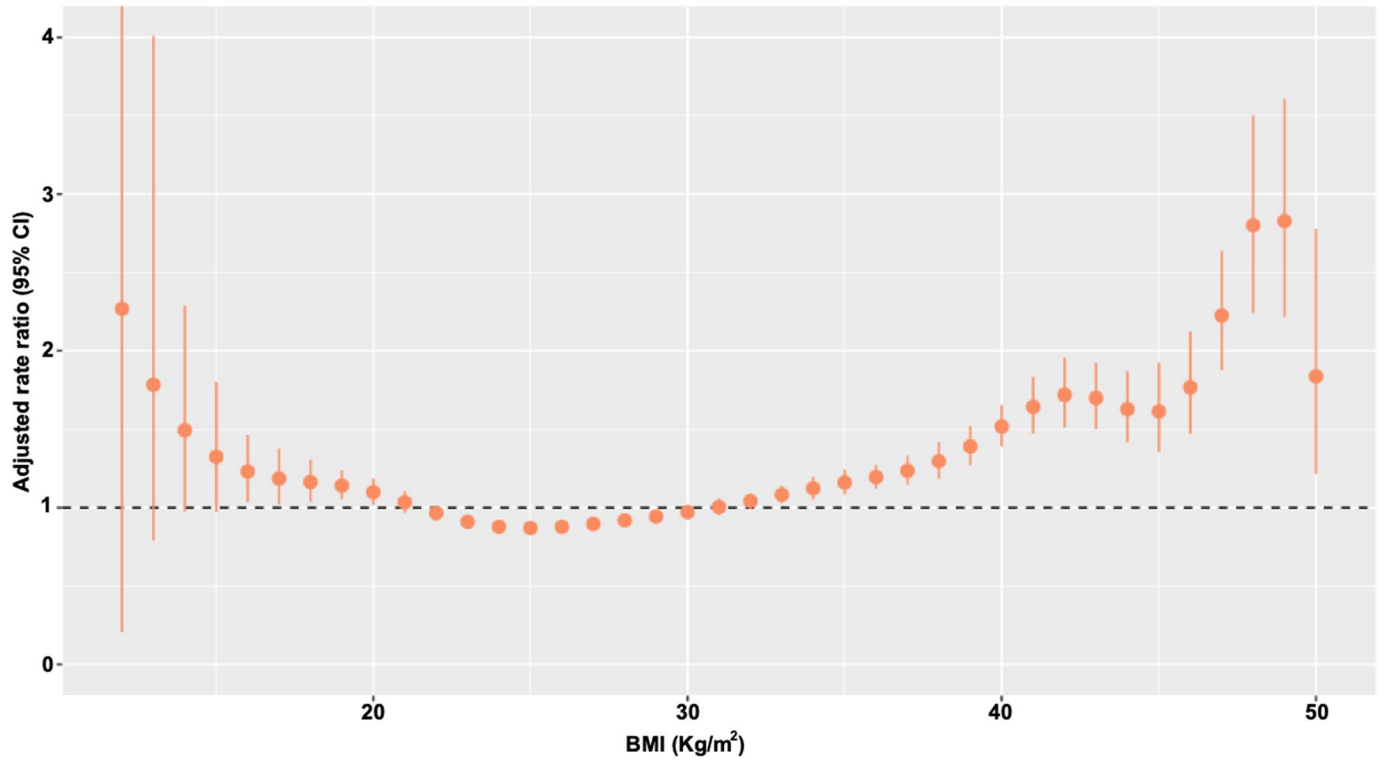
**Peer review information** *Nature Medicine* thanks Melinda Beck, Norio Ohmagari and the other, anonymous, reviewer(s) for their contribution to the peer review of this work. Primary Handling Editor: Jennifer Sargent, in collaboration with the *Nature Medicine* team.

**Reprints and permissions information** is available at [www.nature.com/reprints](http://www.nature.com/reprints).

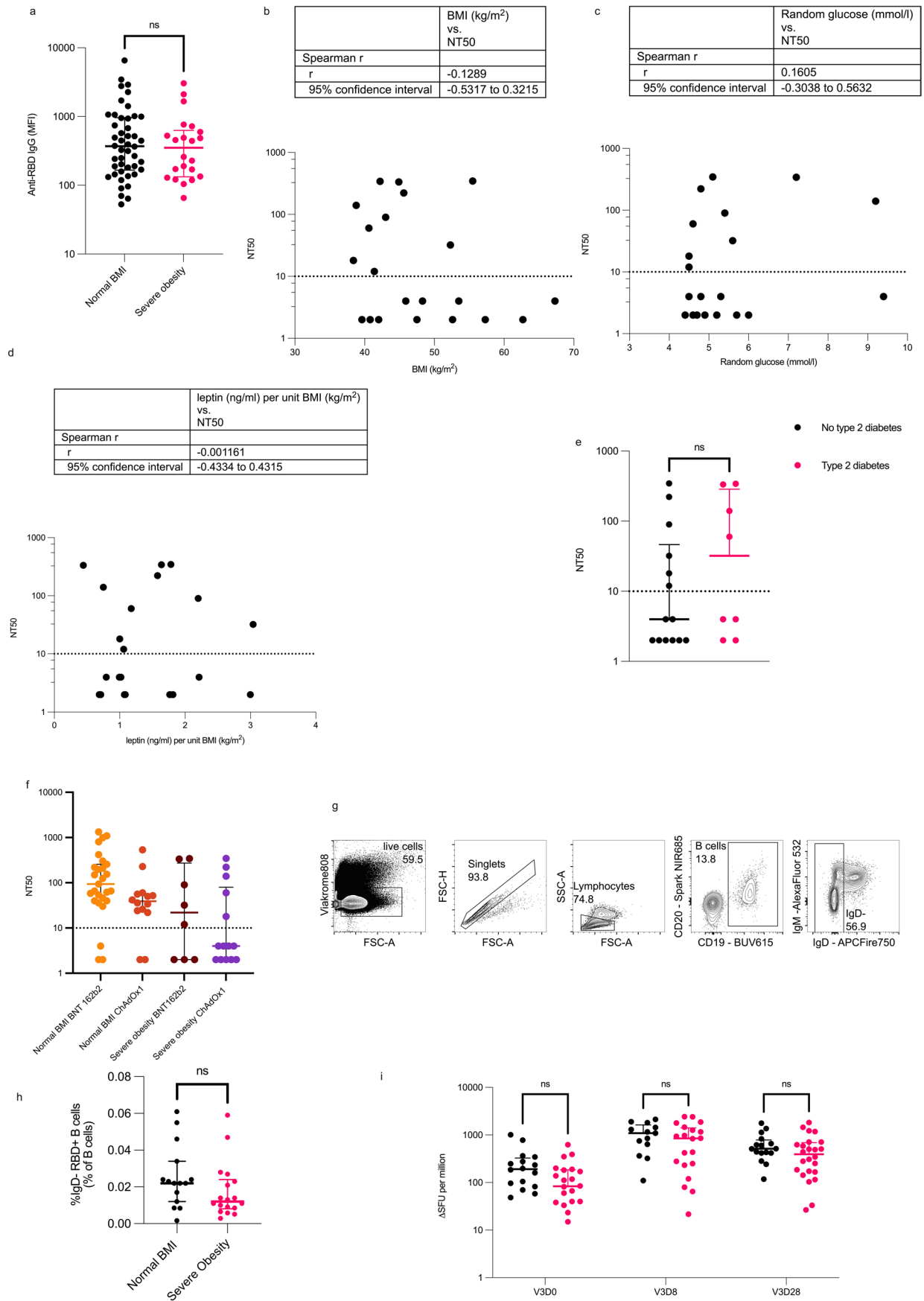


**Extended Data Fig. 1 | Adjusted rate ratios for hospitalization and death due to COVID-19 in vaccinated people. a–e**, Adjusted rate ratios for hospitalization or death following third (booster) doses per BMI category ( $n = 36197$  BMI < 18.5 kg/m<sup>2</sup>,  $n = 456128$  BMI 18.5–24.9 kg/m<sup>2</sup>,  $n = 2428889$  BMI 25–29.9 kg/m<sup>2</sup>,  $n = 568420$  BMI 30–39.9 kg/m<sup>2</sup>,  $n = 98706$  BMI > 40 kg/m<sup>2</sup>). Adjusted Rate Ratios (aRR) for hospitalisation or death following third (booster) dose for different

body mass index (BMI) categories. Error bars indicate 95% confidence intervals. N indicates number of people in each category. **f**, adjusted rate ratios for hospitalisation and death in severely obese individuals with obesity-associated comorbidities ( $n = 98706$  BMI > 40 kg/m<sup>2</sup>). aRR are provided as mean with error bars indicating 95% confidence intervals.



**Extended Data Fig. 2 | Adjusted rate ratios for hospitalization and death due to COVID-19 in vaccinated people using individual BMI values.** Association between BMI ( $\text{kg}/\text{m}^2$ ) as a continuous trait and adjusted rate ratios (with 95% CI, confidence intervals) for severe COVID-19 outcomes. aRR are provided as mean with error bars indicate 95% confidence intervals.

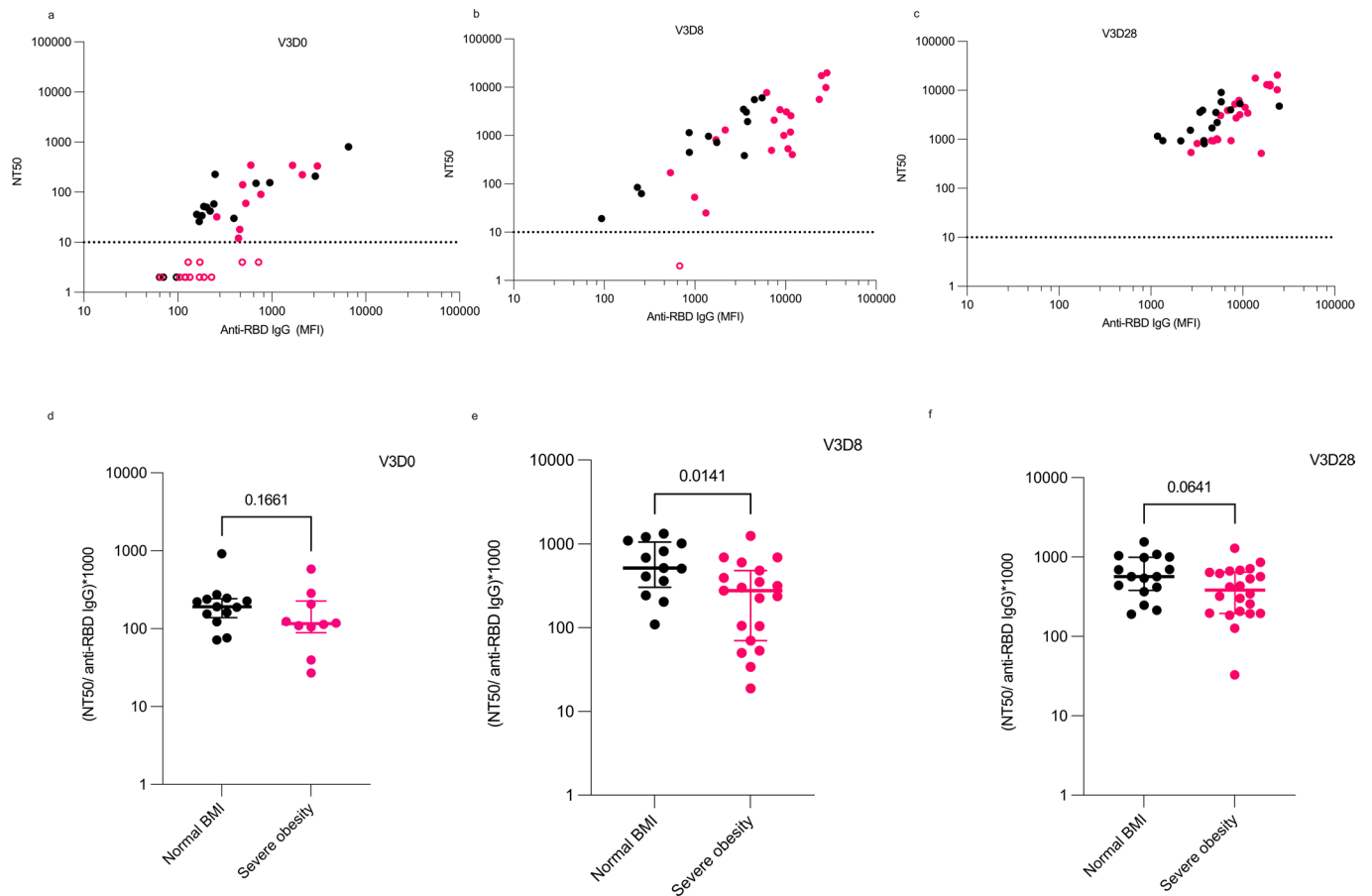


Extended Data Fig. 3 | See next page for caption.



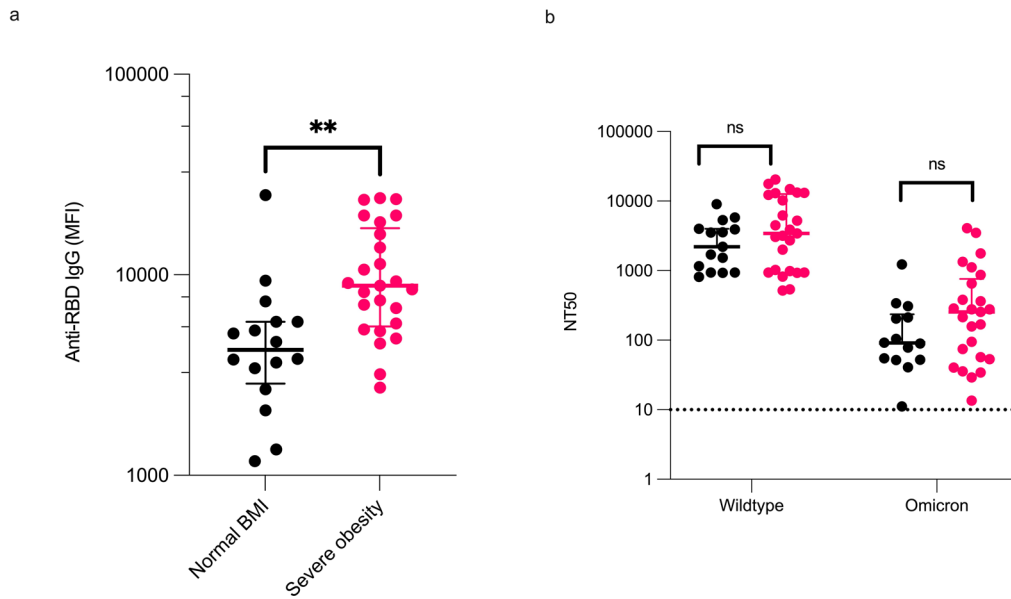
**Extended Data Fig. 3 | SARS-CoV-2 vaccine-induced immunity in people with severe obesity and normal BMI.** **a**, Anti-RBD (receptor binding domain) IgG titres are comparable in 6 months after primary vaccination course ( $P = 0.5801$  in Mann-Whitney U test) in people with severe obesity ( $N = 22$ ) and normal BMI (46). **b-e**, Correlation between body mass index (BMI), random blood glucose, leptin levels per unit BMI in people with severe obesity ( $n = 22$ ) and the presence ( $n = 8$ ) or absence of type 2 diabetes ( $n = 14$ ) and neutralizing capacity (NT50) 6 months after second dose. Non-parametric Spearman's Rho correlations were calculated between NT50 and clinical parameters. Dotted line indicates the limit of quantification. A Mann-Whitney test was used to compare people with severe obesity with and without diabetes mellitus. **f**, Neutralizing capacity (NT50) 6 months after second dose by primary vaccination course - Pfizer-BioNTech BNT162b2 mRNA or AstraZeneca ChAdOx1. Dotted line indicates the limit of

quantification. **g**, shows the B cell Pre-gating used in the flow cytometry analysis. **h**, shows the frequency of antigen-experienced (IgD<sup>-</sup>) Receptor Binding Domain binding (RBD<sup>+</sup>), 6 months after the primary vaccination course; data expressed as a percentage (%) of the total number of B-cells in people with severe obesity ( $n = 15$ ) and normal BMI ( $n = 18$ ). Compared in Mann-Whitney U test. **i**, Antigen-specific T cell responses were measured by ELISpot. Interferon gamma spot forming units (SFU) were quantified. Analysed in mixed effects model. Each symbol represents an individual person and line indicates the median with interquartile range; black symbols indicate people with normal BMI ( $n = 16$ ) and magenta people with severe obesity ( $n = 22$ ). Ns, not significant. V3D0 is before third dose vaccination (V3), V3D8 is 8 days after third dose and V3D28 is 28 days after third dose vaccination.



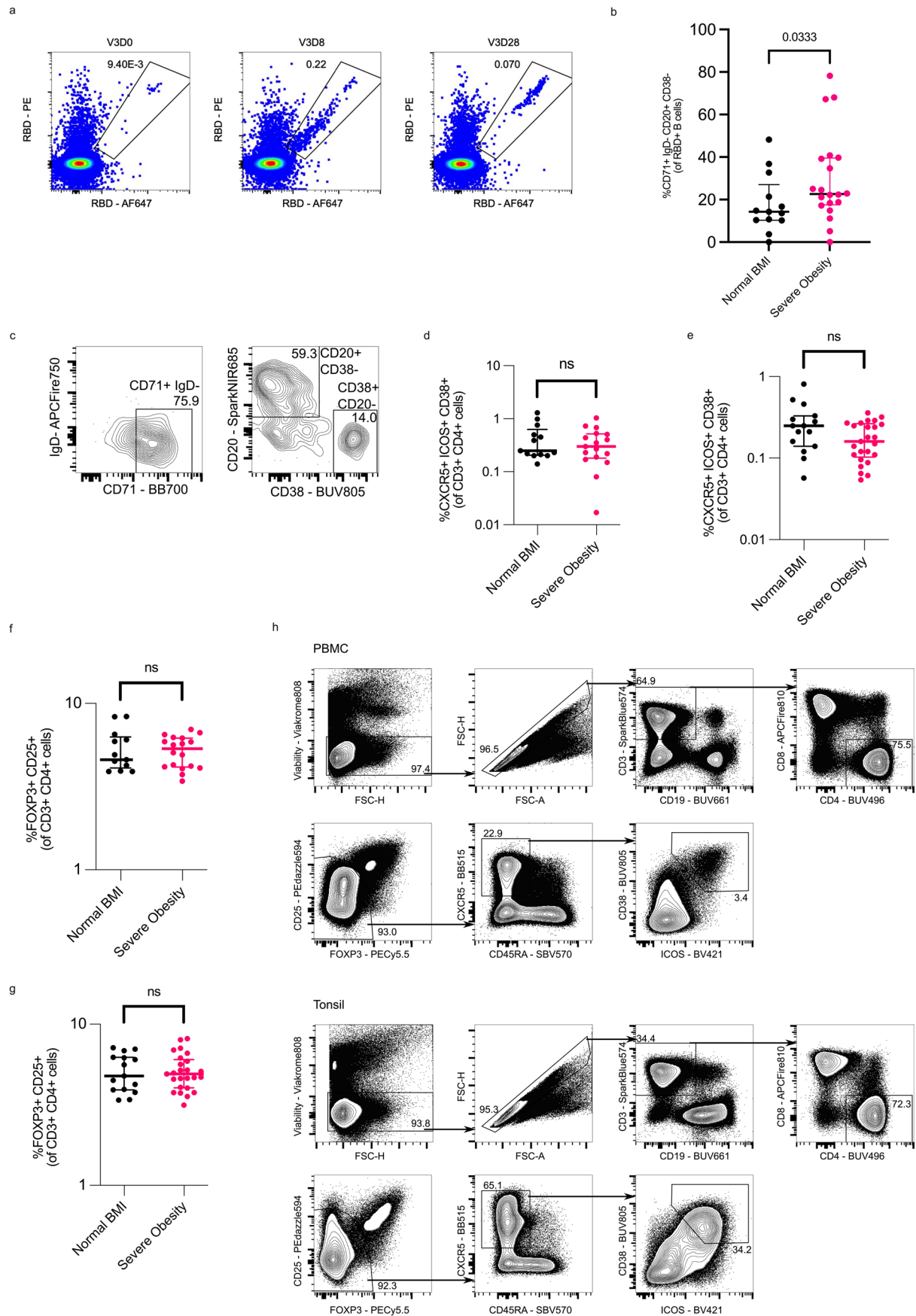
**Extended Data Fig. 4 | Relationship between anti-RBD IgG antibody levels and neutralizing capacity. a-c,** Correlation between NT50 and anti-RBD IgG (MFI) before (V3D0, **a**), 8 days after (V3D8, **b**) and 28 days after (V3D28, **c**) third dose booster vaccination. **d-f,** Ratio of  $(NT50/anti-RBD\ IgG) \times 1000$  before (V3D0, **d**), 8 days after (V3D8, **e**) and 28 days after (V3D28, **f**) third dose booster

vaccination. Each symbol represents an individual person (controls with normal BMI ( $n = 16$ ), black; severe obesity ( $n = 22$ ), magenta). Open symbols represent individuals with unquantifiable or undetectable neutralizing activity. For **d-f**, median values and interquartile ranges are shown. P-values from Mann-Whitney U tests.



**Extended Data Fig. 5 | Response to third dose booster vaccination in severe obesity.** a, Anti-RBD (Receptor Binding Domain) IgG levels (MFI, mean fluorescence intensity) were higher in people with severe obesity (magenta,  $n = 25$ ) compared to individuals with normal BMI (black,  $n = 16$ ) (\*\* $P = 0.0013$  in Mann-Whitney U test). Each symbol represents an individual person studied at Day 28; line indicates the median. b, Neutralizing antibody titres (NT50) against

the Omicron variant of SARS-CoV-2 were markedly reduced compared with wild type virus (Day 28), but no difference was observed between groups (severe obesity (magenta,  $n = 15$ ) compared to normal BMI controls ( $n = 25$ , black)). Each symbol represents an individual person, horizontal bar indicates the median and interquartile range and p-values are from a Mann-Whitney U test. ns, not significant.

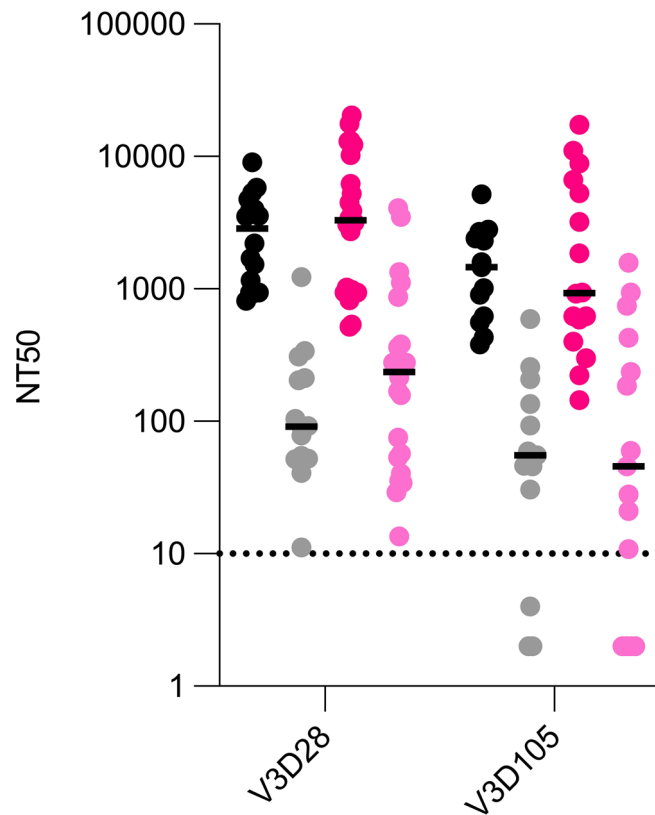


Extended Data Fig. 6 | See next page for caption.



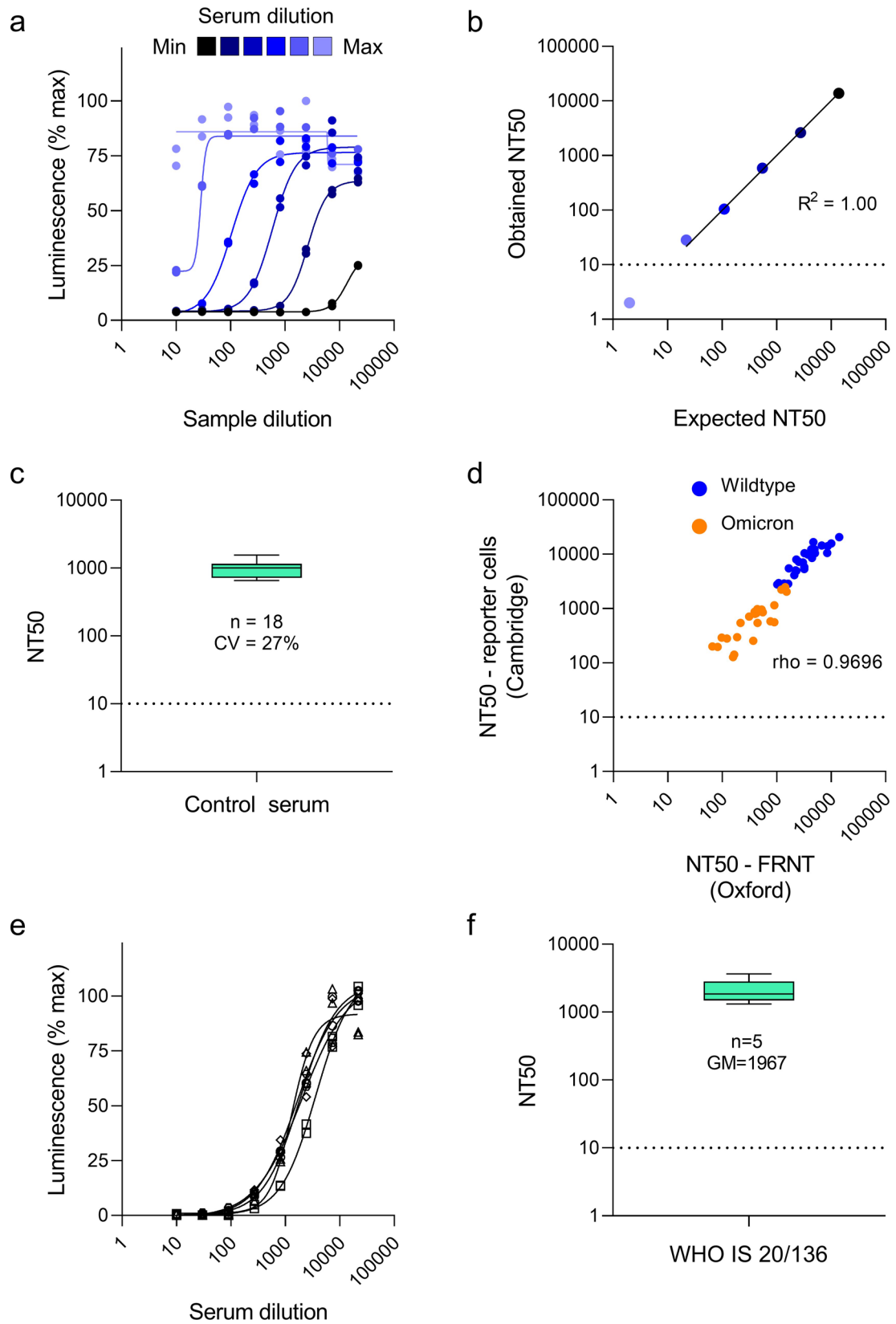
**Extended Data Fig. 6 | B and T cell response to third dose booster vaccination in severe obesity.** **a**, Representative high dimensional spectral flow cytometry analysis in participant with severe obesity. Flow cytometric plots of RBD-binding in a patient with severe obesity, prior to (V3D0), eight days after (V3D8) and 28 days after (V3D28) a booster mRNA vaccine. **b**, Flow cytometric quantification of RBD-binding B cells of activated phenotype in normal BMI individuals (black,  $n = 20$ ) and participants with severe obesity (magenta,  $n = 13$ ) 8 days after (V3D8) a third dose mRNA vaccine. Each symbol represents an individual person, horizontal bars indicate the median and interquartile range and p-value is from a Mann-Whitney U test. \* $P = 0.0333$  **c**, Representative flow cytometric plot-CD71 + IgD CD20 + CD38- gating strategy for S4b. **d-e**, Flow cytometric quantification of circulating T follicular helper (cTfh) cells (CXCR5 + ICOS + CD38 + FOXP3- CD25- CD4 + cells) in normal BMI individuals (black,  $n = 13$  V3D8,  $n = 15$  V3D28) and participants with severe obesity (magenta,  $n = 17$  V3D8,  $n = 25$

V3D28) 8 days (**d**) and 28 days (**e**) after a third dose mRNA vaccine. Each symbol represents an individual person, horizontal bars indicate the median and p-value is from a Mann-Whitney U test. **f-g**, Flow cytometric quantification of circulating T regulatory cells (FOXP3 + CD25 + CD4 + cells) in normal BMI individuals (black,  $n = 13$  V3D8,  $n = 15$  V3D28) and participants with severe obesity (magenta  $n = 18$  V3D8,  $n = 25$  V3D28) 8 days (**f**) and 28 days (**g**) after a third dose mRNA vaccine. **h**, Representative flow cytometry T cell gating, pre-gated on live, single, lymphocytes. Circulating TFH are gated as (CD19- CD20- CD3 + CD4 + FOXP3- CD25- CXCR5 + ICOS + CD38 + ) and T regulatory cells are gated as (CD19- CD20- CD3 + CD4 + FOXP3 + CD25 + ). Tonsil staining was performed alongside PBMC samples to identify bona fide Tfh cells. Each symbol represents an individual person, horizontal bars indicate the median and interquartile range and p-value is from a Mann-Whitney U test.



**Extended Data Fig. 7 | Neutralizing capacity against wildtype and Omicron (BA.1) variant SARS-CoV-2 at day 28 and day 105 post-third dose booster vaccination.** NT50s against wildtype (black and magenta symbols) and Omicron (BA.1) variant SARS-CoV-2 (grey and pink) at day 28 and day 105 post-third

dose booster vaccination in normal BMI individuals (black and grey,  $n = 15$ ) and participants with severe obesity ( $n = 22$ , magenta and pink). Each symbol represents an individual person, horizontal bars indicate medians. Dotted line, limit of quantification.



Extended Data Fig. 8 | See next page for caption.

**Extended Data Fig. 8 | Quality assurance and calibration of assays****for neutralizing antibodies to SARS-CoV-2. a-b**, Linearity of the assay.

Neutralization curves (**a**) and corresponding expected/obtained NT50s (**b**) against wildtype SARS-CoV-2 for a dilution series of high titre positive control serum. Infection of reporter cells is quantified as % maximum luminescence at 16 h. Mean values  $\pm$  SEM are shown for experiments performed in duplicate (**a**). Solid line, line of best fit (dilutions above the limit of quantification).  $R^2$ , coefficient of determination (dilutions above the limit of quantification). Dotted line, limit of quantification. **c**, Precision of the assay. NT50s against wildtype SARS-CoV-2 for a medium titre positive control serum sample from 18 independent experiments are summarised as a Tukey boxplot. CV, inter-assay coefficient of variation. Dotted line, limit of quantification. **d**, External validation of the assay. Comparison of NT50s against both wildtype (blue) and Omicron

(BA.1) variant (orange) SARS-CoV-2 from this paper (reporter cells, Cambridge) with results of Focus Reduction Neutralization Tests (FRNTs, Oxford) for a panel of 28 serum samples from convalescent plasma donors.  $\rho$ , Spearman's rank correlation coefficient. Dotted line, limit of quantification. **e-f**, Calibration of the assay. Neutralization curves (**e**) and corresponding NT50s (**f**) against wildtype SARS-CoV-2 for WHO International Standard 20/136 (WHO IS 20/136) from 5 independent experiments. Infection of reporter cells is quantified as % maximum luminescence at 16 h. Mean values  $\pm$  SEM are shown for experiments performed in duplicate (**e**). NT50s are summarised as a Tukey boxplot (e Minimum: 654, Maximum: 1550, Median: 1006, 25% percentile: 718, 75% percentile: 1157 and f Minimum: 1315, Maximum: 3634, Median: 1851, 25% percentile: 1485, 75% percentile: 2822, Geometric Mean: 1967). GM, geometric mean. Dotted line, limit of quantification.

## Reporting Summary

Nature Portfolio wishes to improve the reproducibility of the work that we publish. This form provides structure for consistency and transparency in reporting. For further information on Nature Portfolio policies, see our [Editorial Policies](#) and the [Editorial Policy Checklist](#).

### Statistics

For all statistical analyses, confirm that the following items are present in the figure legend, table legend, main text, or Methods section.

n/a Confirmed

- The exact sample size ( $n$ ) for each experimental group/condition, given as a discrete number and unit of measurement
- A statement on whether measurements were taken from distinct samples or whether the same sample was measured repeatedly
- The statistical test(s) used AND whether they are one- or two-sided  
*Only common tests should be described solely by name; describe more complex techniques in the Methods section.*
- A description of all covariates tested
- A description of any assumptions or corrections, such as tests of normality and adjustment for multiple comparisons
- A full description of the statistical parameters including central tendency (e.g. means) or other basic estimates (e.g. regression coefficient) AND variation (e.g. standard deviation) or associated estimates of uncertainty (e.g. confidence intervals)
- For null hypothesis testing, the test statistic (e.g.  $F$ ,  $t$ ,  $r$ ) with confidence intervals, effect sizes, degrees of freedom and  $P$  value noted  
*Give  $P$  values as exact values whenever suitable.*
- For Bayesian analysis, information on the choice of priors and Markov chain Monte Carlo settings
- For hierarchical and complex designs, identification of the appropriate level for tests and full reporting of outcomes
- Estimates of effect sizes (e.g. Cohen's  $d$ , Pearson's  $r$ ), indicating how they were calculated

*Our web collection on [statistics for biologists](#) contains articles on many of the points above.*

### Software and code

Policy information about [availability of computer code](#)

Data collection

Data analysis

R (version 3.6.1) was used to carry out all statistical analyses in EAVE II.

All code used in the EAVE II study is publicly available at <https://github.com/EAVE-II/covid-obesity-humoral-response>.

For the SCORPIO study, analysis was completed using GraphPad Prism software version 9.3.1.

tSNE, FlowSOM and heatmap analysis were performed using R (version 4.1.2) using code that has previously been described (Pasciuto, E. et al. Microglia Require CD4 T Cells to Complete the Fetal-to-Adult Transition. Cell 182, 625-640 e624, doi:10.1016/j.cell.2020.06.026 (2020).)

Manual gating of flow cytometry data was performed using FlowJo v10.8 software (Tree Star).

For manuscripts utilizing custom algorithms or software that are central to the research but not yet described in published literature, software must be made available to editors and reviewers. We strongly encourage code deposition in a community repository (e.g. GitHub). See the Nature Portfolio [guidelines for submitting code & software](#) for further information.



## Data

Policy information about [availability of data](#)

All manuscripts must include a [data availability statement](#). This statement should provide the following information, where applicable:

- Accession codes, unique identifiers, or web links for publicly available datasets
- A description of any restrictions on data availability
- For clinical datasets or third party data, please ensure that the statement adheres to our [policy](#)

The study uses established data security principles and processes to keep information secure.

The epidemiology study data that support the findings of this study are not publicly available because they are based on de-identified national clinical records. These are, however, available by application via Scotland's National Safe Haven from Public Health Scotland. The data used in this study can be accessed by researchers through NHS Scotland's Public Benefit and Privacy Panel via its Electronic Data Research and Innovation Service. EAVE II researchers do not have access to view personal medical records, and do not know the identities of any individuals. The information is grouped into broad categories and any information that could identify individuals is removed.

Anonymised data from the SCORPIO study have been included in the manuscript; stored samples are available from the corresponding authors on request.

## Human research participants

Policy information about [studies involving human research participants and Sex and Gender in Research](#).

Reporting on sex and gender

We have reported sex on the participants for both the EAVE II and SCORPIO study.

Population characteristics

The EAVE II cohort contains key information relevant to COVID-19 for almost 5.4 million individuals registered with a general practice (GP) in Scotland – approximately 98-99% of the Scottish population. The EAVE II surveillance platform includes information on clinical and demographic characteristics of each individual, their vaccination status and type of vaccine used and information on positive SARS-COV-2 infection and subsequent hospitalization or death.

Full population characteristics (age, sex, BMI, comorbidities) are described in Table 2 (EAVE II study) and Extended data Table 4 (SCORPIO study).

Recruitment

n/a for the EAVE II Cohort

For the SCORPIO study, participants were recruited from the obesity clinic in Addenbrooke's hospital, Cambridge. All patients in the obesity clinic were approached over the recruitment period of SCORPIO. As referral to the clinic is based on severity of obesity (BMI > 35 kg/m<sup>2</sup> with one or more obesity-related comorbidities or BMI > 40 kg/m<sup>2</sup>), this means that results obtained in this group may not be generalisable to individuals with mild or moderate obesity. People with acquired (HIV, immunosuppressant drugs) or congenital immune deficiencies and cancer were excluded which means results will not be generalisable to people with obesity and those conditions. Given the set up of multiple visits over a short period of time, participants with severe mobility issues due to their obesity, living at greater distance from the hospital, inflexible work or care commitments were less likely to consent to participate. The participants with normal BMI were recruited through advertisement in Cambridge University departmental emails and through the PITCH study which is a cohort of health care workers. Inclusion criteria were: no comorbidities, normal BMI and thus selected a relatively fit and healthy group.

Ethics oversight

1. EAVE II has been given approval from:

Ethical approval was granted by the National Research Ethics Service Committee, Southeast Scotland 02 (reference number: 12/SS/0201) for the study using the Early Pandemic Evaluation and Enhanced Surveillance of COVID-19 (EAVE II) platform. Approval for data linkage was granted by the Public Benefit and Privacy Panel for Health and Social Care (reference number: 1920-0279). Individual written patient consent was not required for this analysis.

2. The SCORPIO study has been given approval from:

1) Clinical studies in people with severe obesity and normal BMI controls were approved by the National Research Ethics Committee and Health Research Authority (East of England – Cambridge Research Ethics Committee (SCORPIO study, SARS-CoV-2 vaccination response in obesity amendment of "NIHR BioResource" 17/EE/0025)). Each participant provided written informed consent. All studies were conducted in accordance with the Declaration of Helsinki.

2) Additional normal BMI controls were recruited in Oxford, UK as part of the PITCH study under the GI Biobank Study 16/YH/0247, approved by Yorkshire & Humber Sheffield Research Ethics Committee, which was amended for this purpose on 8 June 2020.

3) For external validation of assays for neutralizing antibodies, a panel of serum samples from the C-VELVET study (approved by the West Midlands Solihull Research Ethics Committee, REC reference: 21/WM/0082, IRAS project ID: 296926) was tested.

Note that full information on the approval of the study protocol must also be provided in the manuscript.

## Field-specific reporting

Please select the one below that is the best fit for your research. If you are not sure, read the appropriate sections before making your selection.

Life sciences       Behavioural & social sciences       Ecological, evolutionary & environmental sciences

For a reference copy of the document with all sections, see [nature.com/documents/nr-reporting-summary-flat.pdf](https://www.nature.com/documents/nr-reporting-summary-flat.pdf)

## Life sciences study design

All studies must disclose on these points even when the disclosure is negative.

Sample size	Not applicable for EAVE II as this is a large population level based study; N/A for SCORPIO as this is an exploratory case-control study.
Data exclusions	Data from participants in the SCORPIO study who tested positive for SARS-CoV-2 infection by RT-PCR was excluded. Missing data in addition to this were due to 1) occasional difficult venepuncture in people with obesity, 2) insufficient PBMCs were isolated for both T and B cell analysis or 3) insufficient sample to run both WT and omicron neutralization assays. Therefore, we have specified how many participants were included per analysis/ per figure.
Replication	This is not applicable for both studies. There is no similar cohort available to replicate the EAVE II studies. Similarly it was not possible to replicate the case-control SCORPIO study. Some of the immunogenicity markers were performed in technical duplicates (quantification of neutralising antibodies to SARS-CoV-2).
Randomization	The SCORPIO case-control study was not randomized. Severely obese cases and normal BMI controls were defined by BMI criteria.
Blinding	Researchers conducting immunoassays used samples that were fully anonymised and as such were blinded to the case vs control status of participants.

## Reporting for specific materials, systems and methods

We require information from authors about some types of materials, experimental systems and methods used in many studies. Here, indicate whether each material, system or method listed is relevant to your study. If you are not sure if a list item applies to your research, read the appropriate section before selecting a response.

### Materials & experimental systems

n/a	Involved in the study
<input type="checkbox"/>	<input checked="" type="checkbox"/> Antibodies
<input type="checkbox"/>	<input checked="" type="checkbox"/> Eukaryotic cell lines
<input checked="" type="checkbox"/>	<input type="checkbox"/> Palaeontology and archaeology
<input checked="" type="checkbox"/>	<input type="checkbox"/> Animals and other organisms
<input type="checkbox"/>	<input checked="" type="checkbox"/> Clinical data
<input checked="" type="checkbox"/>	<input type="checkbox"/> Dual use research of concern

### Methods

n/a	Involved in the study
<input checked="" type="checkbox"/>	<input type="checkbox"/> ChIP-seq
<input type="checkbox"/>	<input checked="" type="checkbox"/> Flow cytometry
<input checked="" type="checkbox"/>	<input type="checkbox"/> MRI-based neuroimaging

## Antibodies

Antibodies used

The following antibodies were used:

BUV395 Mouse Anti-Human CD27, Clone L128, BD Biosciences, cat# 563816, AB\_2744349  
 CD57 Antibody (TB01) [Alexa Fluor® 350], Clone TB01, Novus Biologicals, cat# NBP2-62203AF350, AB\_2909528  
 Hu CD4 BUV496 M-T477 50ug, BD Biosciences, cat# 750175, AB\_2874380  
 BUV563 Mouse Anti-Human FCRL5 (CD307e), Clone 509F6, BD Biosciences, cat# 749598, AB\_2873900  
 BUV615 Mouse Anti-Human CD19, Clone H1B19, BD Biosciences, cat# 751273, AB\_2875287  
 BUV661 Mouse Anti-Human CD11c, Clone B-ly6, BD Biosciences, cat# 612967, AB\_2870241  
 BUV737 Mouse Anti-Human CD10, Clone H110a, BD Biosciences, cat# 741825, AB\_2871160  
 BUV805 Mouse Anti-Human CD38, Clone HB7, BD Biosciences, cat# 742074, AB\_2871359  
 Brilliant Violet 421™ anti-human/mouse/rat CD278 (ICOS) Antibody, Clone C398.4a, Biolegend, cat# 313524, AB\_2562545  
 T-bet Monoclonal Antibody (eBio4B10 (4B10)), eFluor™ 450, eBioscience™, Clone 4B10, Thermo Fisher Scientific, cat# 48-5825-82, AB\_2784727  
 BV480 Mouse Anti-Human CD21, Clone B-ly4, BD Biosciences, cat# 746613, AB\_2743893  
 BV510 Mouse Anti-Human TCR γδ, Clone B1, BD Biosciences, cat# 740179, AB\_2739932  
 MOUSE ANTI HUMAN CD45RA:StarBright Violet 570, Clone F8-11-13, Bio-Rad, cat# MCA885BV570, AB\_871980  
 BV650 Mouse Anti-Human CD183, Clone 1C6/CXCR3, BD Biosciences, cat# 740603, AB\_2740303  
 BV711 Mouse Anti-GATA3, Clone L50-823, BD Biosciences, cat# 565449, AB\_2739242

BV750 Mouse Anti-Human CD279 (PD-1), Clone EH12.1, BD Biosciences, cat# 747446, AB\_2872125  
 BV786 Mouse Anti-Human HLA-DR, Clone G46-6, BD Biosciences, cat# 564041, AB\_2738559  
 BB515 Rat Anti-Human CXCR5 (CD185), BD Biosciences, cat#564624, AB\_2738871  
 IgM Antibody (IM373) [Alexa Fluor® 532], Clone IM373, cat# NBP2-34650AF532, AB\_2909529  
 Spark Blue™ 550 anti-human CD3 Antibody, Clone SK7, BioLegend, cat# 344851, AB\_2819984  
 CD14 Monoclonal Antibody (61D3), PerCP-Cyanine5.5, eBioscience™, Clone 61D3, Thermo Fisher Scientific, cat# 45-0149-42, AB\_1518736  
 CD196 (CCR6) Monoclonal Antibody (R6H1), PerCP-eFluor™ 710, eBioscience™, Clone R6H1, Thermo Fisher Scientific, cat# 46-1969-42, AB\_10597900  
 BB700 Mouse Anti-Human CD71, Clone M-A712, BD Biosciences, cat# 746082, AB\_2743458  
 IRF4-BB790, Clone Q9-343, BD Biosciences, custom conjugation  
 Spark YG™ 593 anti-mouse/human CD11b Antibody, Clone M1/70, BioLegend, cat# 101282, AB\_2892261  
 Alexa Fluor® 594 anti-human CD44 Antibody, Clone C44Mab-5, BioLegend, cat# 397509, AB\_2860987  
 PE/Dazzle™ 594 anti-human CD25 Antibody, Biolegend, Cat# 302646, AB\_2734260  
 CD24 Monoclonal Antibody (SN3), PE-Alexa Fluor™ 610, Clone SN3, Thermo Fisher Scientific, cat# MHCD2422, AB\_1468089  
 PE/Cyanine5 anti-human CD184 (CXCR4) Antibody, Clone 12G5, BioLegend, cat# 306508, AB\_314614  
 FOXP3 Monoclonal Antibody (FJK-16s), PE-Cyanine5.5, eBioscience™, Clone FJK-165, Thermo Fisher Scientific, cat# 35-5773-82, AB\_11218094  
 ROR gamma (t) Monoclonal Antibody (B2D), PE-Cyanine7, eBioscience™, Clone B2D, Thermo Fisher Scientific, cat# 25-6981-82, AB\_2784671  
 PE/Fire™ 810 anti-human CD197 (CCR7) Antibody, Clone G043H7, BioLegend, cat# 353269, AB\_2894572  
 Spark NIR™ 685 anti-human CD20 Antibody, Clone 2H7, BioLegend, cat# 302366, AB\_2860775  
 Ki-67 Monoclonal Antibody (Sola15), Alexa Fluor™ 700, eBioscience™, Clone Sola15, Thermo Fisher Scientific, cat# 56-5698-82, AB\_2637480  
 ViaKrome 808 Fixable Viability Dye, Beckman Coulter, cat# C36628  
 APC/Fire™ 750 anti-human IgD Antibody, Clone IA6-2, BioLegend, cat# 348238, AB\_2616988  
 APC/Fire™ 810 anti-human CD8 Antibody, Clone SK1, BioLegend, cat# 344764, AB\_2860890  
 Biotinylated detection mAb 7-B6-1, Mabtech, cat# 3420-4APT-10, Batch 56.3  
 Anti-human IgG Fc Specific – PE, Clone HP6043, Leinco Technologies, Inc., cat# I-127

Specific dilutions are included in supplementary table 9.

#### Validation

All antibodies used are commercially available antibodies and validated by the supplier.

## Eukaryotic cell lines

Policy information about [cell lines and Sex and Gender in Research](#)

#### Cell line source(s)

Luminescent HEK293T reporter cells for SARS-CoV-2 were generated in the Matheson lab as previously described (<https://doi.org/10.1371/journal.ppat.1010265>). They are available from the National Institute for Biological Standards and Control (NIBSC, [www.nibsc.org](http://www.nibsc.org), catalogue number 101062).

#### Authentication

HEK293T cells were authenticated by STR profiling as previously described (<https://doi.org/10.1371/journal.ppat.1010265>).

#### Mycoplasma contamination

Luminescent HEK293T reporter cells for SARS-CoV-2 were regularly screened and confirmed to be mycoplasma negative (Lonza MycoAlert and IDEXX BioAnalytics).

#### Commonly misidentified lines (See [ICLAC](#) register)

No commonly misidentified lines were used.

## Clinical data

Policy information about [clinical studies](#)

All manuscripts should comply with the ICMJE [guidelines for publication of clinical research](#) and a completed [CONSORT checklist](#) must be included with all submissions.

#### Clinical trial registration

This is not a clinical trial and as such does not require trial registration. Below are the relevant ethical approvals for the different arms of the study.

#### Study protocol

This is not a clinical trial and has no trial protocol.

#### Data collection

The EAVE II surveillance platform drew on near real-time nationwide health care data for 5.4 million individuals (~99%) in Scotland. It includes information on clinical and demographic characteristics of each individual, their vaccination status and type of vaccine used and information on positive SARS-CoV-2 infection and subsequent hospitalization or death.

The SCORPIO study recruited people with severe obesity (class II/ III WHO criteria of BMI  $\geq 40$  kg/m<sup>2</sup> or BMI  $\geq 35$  kg/m<sup>2</sup> with obesity-associated medical conditions such as type 2 diabetes, hypertension) who attended the obesity clinic at Cambridge University Hospitals NHS Trust and had received two doses of SARS-CoV-2 vaccination (first and second dose of ChAdOX1 nCoV-19 or BNT162b2 mRNA) between December 2021 and May 2022. Clinical and immunological measurements were taken before the third dose booster vaccination, 8 (-3) days, 28 (+7) days and 105 (+7) days after vaccination.

#### Outcomes

EAVE II study outcomes: The cohort analysed for this study consisted of individuals aged 18 and over who were administered with at least two doses of BNT162b2 mRNA, ChAdOX1 nCoV-19 or mRNA-1273 vaccines. Follow-up began 14 days after receiving the second dose until Covid-19 related hospitalization, Covid-19 related death or the end of study period. The primary outcome of interest was severe Covid-19, which was defined as Covid-19 related hospital admission or death, 14 days or more after receiving the second

vaccine or booster dose.

Outcomes SCORPIO study: The measurement of humoral immunity using serology, live virus neutralisation capacity, B and T cell immunity were the primary outcomes in the SCORPIO study.

## Flow Cytometry

### Plots

Confirm that:

- The axis labels state the marker and fluorochrome used (e.g. CD4-FITC).
- The axis scales are clearly visible. Include numbers along axes only for bottom left plot of group (a 'group' is an analysis of identical markers).
- All plots are contour plots with outliers or pseudocolor plots.
- A numerical value for number of cells or percentage (with statistics) is provided.

### Methodology

Sample preparation

Peripheral blood samples were acquired in lithium heparin tubes from participants in the SCORPIO study. Peripheral blood mononuclear cells (PBMCs) were isolated by layering over lymphoprep density gradient medium (Stemcell Technologies) followed by density gradient centrifugation at 800 x g for 20 minutes at RT. PBMCs were isolated and washed twice using wash buffer (1X PBS, 1% foetal calf serum, 2mM EDTA) at 400 x g for 10 minutes at 4°C. Isolated PBMCs were resuspended in freezing media, aliquoted and stored at -80°C for up to a week before being transferred to liquid nitrogen until use. For using in flow cytometry 1mL PBMC samples were defrosted in a 37°C water bath, and then immediately diluted into 9mL of pre-warmed RPMI+10% Fetal Bovine serum (FBS). Cells were washed twice with 10 mL of FACS buffer (PBS containing 2% FBS and 1mM EDTA). Cells were then resuspended in 500uL of FACS buffer and cell numbers and viability were determined using a Countess™ automated cell counter (Invitrogen). 5x10<sup>6</sup> viable cells were transferred to 96-well plates for antibody staining. Cells were then washed once with FACS buffer, and stained with 100 µL of surface antibody mix (including B cell probes) for 2 hours at 4°C. Cells were then washed twice with FACS buffer, and fixed with the eBioscience Fcγ3/Transcription Factor Staining Buffer (ThermoFisher #00-5323-00) for 30 min at 4°C. Cells were then washed with 1x eBioscience Fcγ3/Transcription Factor Permeabilisation buffer (ThermoFisher #00-801 8333-56) twice and stained with intracellular antibody mix in permeabilisation buffer at 4°C overnight. Following overnight staining, samples were washed twice with 1x permeabilisation buffer and once with FACS buffer before analysis.

Instrument

Cytek™ Aurora

Software

FlowJo v10.8 software

Cell population abundance

Not applicable as no cell sorting was used.

Gating strategy

Data presented as % of total lymphocytes or % of B cells.  
 Prior gating strategy: Live (viability dye negative), singlets (fsc-a / fsc-h), B cells (CD19+ CD20+)  
 Extended data figures 3 and 6 contain pre-gating + full gating strategies for the above populations, as well as circulating TFH full gating strategy.

- Tick this box to confirm that a figure exemplifying the gating strategy is provided in the Supplementary Information.